Supplementary Information for

# Leveraging the bioeconomy for carbon drawdown

John P. Dees,[a] William Joe Sagues,[b,c] Ethan Woods,[b] Hannah M. Goldstein,[d] A.J. Simon,[d] Daniel L. Sanchez[e*]

**Author Information:**
[a]Energy and Resources Group, University of California, Berkeley, Berkeley, CA, 94720, USA
b Department of Biological & Agricultural Engineering, North Carolina State University, Raleigh, NC, 27695, USA
[c]National Renewable Energy Laboratory, FTLB Lab, 16253 Denver West Parkway, Golden, CO 80401, USA
[d]Lawrence Livermore National Laboratory, 7000 East Avenue, Livermore, CA, 94550, USA
[e]Environmental Science, Policy, and Management (ESPM), University of California, Berkeley, Berkeley, CA, 94720, USA
*Correspondence and requests for materials should be addressed to Dan Sanchez:

Department of Environmental Science, Policy, & Management, UC Berkeley, 130 Mulford Hall, #3114, Berkeley, CA 94720, Email: sanchezd@berkeley.edu

The supplementary information in subsequent sections provides a detailed explanation of the methods used to derive 10,000-year estimates of carbon sequestration (S1) and the life cycle GHG emissions of the four biomass conversion pathways analyzed (S2.3 - S2.6). A more complete exposition of analysis results, combining the cradle-to-gate analyses in (S2) with the long-term sequestration estimates in (S1) is presented for switchgrass IGCC with CCS (S2.3.2), corn stover polyethylene with CCS (S2.4.2), biochar from forest residues (S2.5.2), and oriented strand board from forest residues (S2.6.2).

## S1 Sequestration technologies

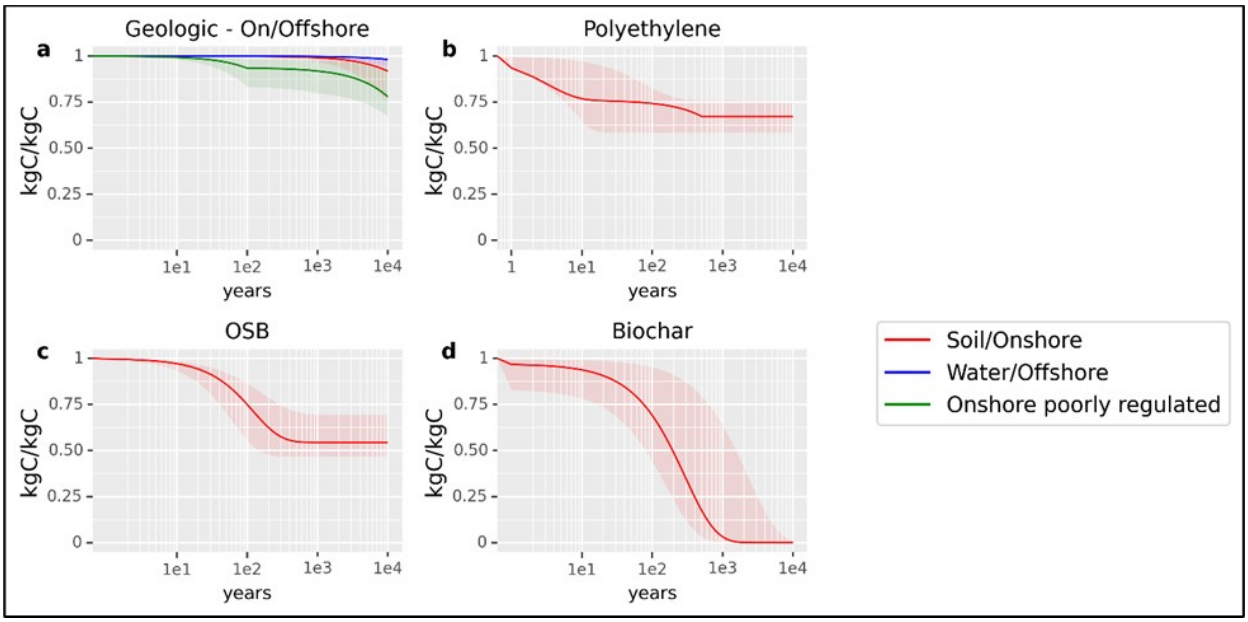


**Fig. S1**– Estimated carbon sequestration over 10,000 years. This figure illustrates a range of optimistic, pessimistic, and moderate cases for carbon sequestration over time. The dark red line in each panel is the moderate estimate for each analyzed scenario. The dark blue and dark green lines in panel (a) represent the P50 estimate (see S1.1) for offshore and onshore poorly-regulated geologic sequestration. The dark red line in panel (a) is the P50 scenario for onshore, well-regulated wells. This is the baseline case for geological sequestration in this analysis. The functional form in each case considers a pulse of carbon entering the carbon cycle in the form of a product or sequestration co-product. From the production gate, the function may consider (where appropriate) operational use-life, recycling, secondary use, and sequestration of carbon in the product or biosphere. Panels: **a.** Geologic sequestration of industrially captured $CO_2$ in either onshore well-regulated or poorly-regulated or offshore well-regulated reservoirs **b.** carbon sequestered in a polyethylene product. Note that the discontinuity and shape of the function results from the interaction of both linear (landfill decay) and exponential (use-life decay) components in the function. **c.** carbon sequestered in oriented strand board (OSB) construction material **d.** carbon sequestered in biochar soil ammendment applied to agricultural soil.

## S1.1 Geological Storage

Our estimates are adapted from Alcalde et al. (2018)[1], who used a Monte Carlo modeling approach to estimate $CO_2$ leakage from geologic reservoirs over 10,000 years. The analysis considers well-regulated onshore and offshore wells and poorly regulated wells (onshore only). **Table S1** shows the 5$^{th}$, 50$^{th}$, and 95$^{th}$ percentile thresholds for the % of $CO_2$ leaked at the time in years. P95 indicates that 95% of the values in model runs were greater than that value. P5 indicates that 5% of the model runs returned values greater than the indicated value.

**Table S1** – Percentage of geologically sequestered carbon leakage over time (adapted from Alcalde et al. (2018)

| **Time since sequestration (years)** | **Onshore Geological (Well-regulated) – $CO_2$ leaked (%)** | | | **Offshore Geological (Well-regulated) - – $CO_2$ leaked (%)** | | | **Onshore Geological (Poorly-regulated) - – $CO_2$ leaked (%)** | | |
|---|---|---|---|---|---|---|---|---|---|
| | P95 | P50 | P5 | P95 | P50 | P5 | P95 | P50 | P5 |
| 1 | 0.0013 | 0.0022 | 0.0045 | 0.0005 | 0.0008 | 0.0014 | 0.0517 | 0.202 | 0.521 |
| 100 | 0.0737 | 0.156 | 0.358 | 0.0249 | 0.0447 | 0.0888 | 1.70 | 6.41 | 16.5 |

| | | | | | | | | | |
|---|---|---|---|---|---|---|---|---|---|
| 1000 | 0.246 | 0.888 | 2.96 | 0.0709 | 0.213 | 0.646 | 2.39 | 8.05 | 20.0 |
| 10000 | 1.81 | 8.18 | 25.71 | 0.483 | 1.89 | 6.29 | 6.91 | 22.0 | 32.6 |

We convert the leakage values in **Table S1** to % $CO_2$ (or % carbon) remaining sequestered by subtracting each cell from 100 (**Table S2**). P95 now indicates that 95% of values are less than the indicated value while P5 indicates that 5% of modeled values are less than the indicated value.

**Table S2** – Percentage of carbon remaining geologically sequestered over time.

| **Time since sequestration (years)** | **Onshore Geological (Well-regulated) – $CO_2$ remaining in storage (%)** | | | **Offshore Geological (Well-regulated) – $CO_2$ remaining in storage (%)** | | | **Offshore Geological (Poorly-regulated) – $CO_2$ remaining in storage (%)** | | |
|---|---|---|---|---|---|---|---|---|---|
| | P95 | **P50** | P5 | P95 | P50 | P5 | P95 | P50 | P5 |
| 1 | 99.9987 | **99.9978** | 99.9955 | 99.9995 | 99.9992 | 99.9986 | 99.9483 | 99.798 | 99.479 |
| 100 | 99.9263 | **99.844** | 99.642 | 99.9751 | 99.9553 | 99.9112 | 98.3 | 93.59 | 83.5 |
| 1000 | 99.754 | **99.112** | 97.04 | 99.9291 | 99.787 | 99.354 | 97.61 | 91.95 | 80 |
| 10000 | 98.19 | **91.82** | 74.29 | 99.517 | 98.11 | 93.71 | 93.09 | 78 | 67.4 |

We fit a first-order decay function to the P95, P50, and P5 values to calculate % $CO_2$ remaining sequestered at any time (t) where *r* is the decay rate. The onshore and offshore well-regulated cases are modeled with single decay function and rate. The onshore poorly regulated case is modeled with three different decay rates for 0-100; 101-1,000; and 1001-10,000 years in each of the probability divisions.

Eq. 1

$$C_{geo}(t) = C_0 e^{-rt}$$

The decay function matches the Monte Carlo results within < 1% in each referenced period. This is the function reported in **Fig. S1a** , with P95, P50, and P5 for both onshore and offshore representing optimistic, midrange, and pessimistic bounds, respectively.

In the life cycle analyses in Part II of our paper, we estimate the emissions from geological sequestration in the IGCC and polyethylene pathways from the onshore, well-regulated scenario only.

## S1.2 Carbon sequestered in polyethylene and landfills

We model the sequestration of carbon in plastic goods as a multi-stage process, including a use phase, a recycling or up-cycling phase, and eventual end-of-life (EOL) as waste in a managed or unmanaged environment or as a feedstock for energy production. We consider only the most common EOL pathways in the U.S. Using 2017 estimates from the EPA[2], we assume that 8% of

polyethylene is recycled, 16% is combusted, and 76% enters landfills. To represent optimistic, moderate, and pessimistic cases for polyethylene (PE) carbon in landfills (**Fig. S1b**), we consider low-density polyethylene (LDPE) grocery bags, high-density polyethylene (HDPE) bottles, and HDPE water pipe, respectively. We conservatively assume a 2-year half-life in use for a given stock of LDPE bags or HDPE bottles. Industry literature reports that HDPE pipe can last as long as 100 years.[3] We assume a 50-year half-life to represent the use phase for a given stock of HDPE pipe. The use phase stock ($PE_{UL}$) of carbon remaining in polyethylene from a production pulse of PE ($PE_0$) is estimated by a first-order decay function of the form:

Eq. 2

$$PE_{UL}(t) = PE_0 e^{-rt}$$

Where *r* is the decay rate determined by the half-life and *t* is time.

As a pulse of PE exits its use-life, it may be recycled, combusted for energy, or it enters a managed landfill (we only consider "best management practices"). Recycled plastics are typically processed into a lower grade product than the original product. However, for simplicity, we track the carbon sequestered in recycled plastics by adding the carbon back to the stock at each time *t*. Combusted PE is assumed to release all carbon as $CO_2$.

Determining the degradation rate of carbon stored in PE once it reaches landfill is challenging due to a wide variety of environmental conditions and the timescales required to observe degradation in field settings. However, indirect methods (e.g. accelerated degradation) as well as extrapolations from short-duration experiments do offer some insight.

Conventional greenhouse gas accounting of municipal solid waste as adopted by the U.S. EPA assumes that the carbon in plastics in landfills is permanently sequestered.[4–6] However, studies have indicated the potential for plastics such as PE to break down into mineralized carbon under the conditions found in a landfill environment.[7,8] In order to be released as landfill gasses via biodegradation, highly stable PE would first need to undergo chemical decomposition via physical processes (photodegradation from UV light, thermo-oxidation, and hydrolysis).[9] Degradation rates are subject to a number of environmental factors (temperature, humidity, pH, presence of oxygen).

In our analysis, we do not attempt to model biodegradation and instead adopt a physical decay model as a proxy. We implement a zeroth-order linear decay model based on physical processes as adapted from Chamas et al. (2020).[10] Physical degradation is a function of surface area and material density.[10] We assume that between 1% and 23% of the carbon in landfilled PE is subject to decay. The upper bound of 23% is a somewhat arbitrary and conservative limit based on the labile fraction assumption for harvest wood products[11] while the lower bound of 1% approximates the EPA assumption. We selected a simple midpoint of 11.5% for the moderate case. Chamas et al. (2020) reports a range of degradation half-lives from the literature for LDPE bags, HDPE bottles, and HDPE pipe degrading in soil: 4.6 years, 230-280 (250) years, and

4,600-5,500 (5,000) years, respectively. The half-lives in parenthesis (and the 4.6 years for LDPE bags) are the estimates modeled by Chamas et al. (2020). We calculate decay rates from these half-lives.

We then calculate the quantity of carbon remaining sequestered in PE in use or in landfills at any time $t$ = 1 to 10,000 years (**Fig. S1b**), where:

The proportion of PE carbon in use-life at any time *t*:

If $PE_{UL}(0) = 1$ then $PE_{UL}(t)$ can be sequentially calculated to account for recycling:

Eq. 3

$$PE_{UL}(t) = PE_{UL}(t-1)e^{u} + [0.08\left(PE_{UL}(t-1) - PE_{UL}(t-1)e^{u}\right)]$$

Where $u$ is the use-life decay rate and the portion of the function in the brackets is equal to the recycled fraction (8%) of PE leaving use-life at any time *t.*

Or:

Eq. 4 $$PE_{UL}(t) = PE_{UL}(t-1)[e^{u} + 0.08[1 - e^{u}]]$$

The pulse of PE carbon exiting use-life at any time *t*:

Eq. 5

$$PE_{W}(t) = PE_{UL}(t-1) - PE_{UL}(t)$$

And entering landfills:

Eq. 6

$$PE_{New}(t) = 0.76PE_{W}(t)$$

The carbon remaining sequestered in the landfills at any time *t:*

Eq. 7

$$PE_{LF}(t) = \sum_{i=1}^{t} f_{labile}PE_{New}(i)(1 - r(t-i)) + f_{recalc}PE_{New}(i)$$

where $r$ is the linear decay rate of the PE in landfills, and $f_{labile}$ and $f_{recalc}$ represent the labile and recalcitrant fractions of carbon, respectively.

Total carbon remaining sequestered at any time *t:*

Carbon sequestered at time $t$ is the sum of the fraction of carbon remaining in its useful life and the fraction remaining sequestered in the landfill.

Eq. 8

$$PE_{seq}(t) = PE_{UL}(t) + PE_{LF}(t)$$

The fraction of carbon remaining in PE and landfills at time t is shown in **Fig. S1b**. The estimated carbon loss to the atmosphere in each case is shown in **Table S3.**

**Table S3** - Percentage of polyethylene and landfill carbon loss to atmosphere over time. Values in bold-face reflect moderate case assumptions used in the main text.

| Time since sequestration (years) | Carbon loss from polyethylene and landfills (%) - Optimistic | Carbon loss from polyethylene and landfills (%) - Moderate | Carbon loss from polyethylene and landfills (%) - Pessimistic |
|---|---|---|---|
| 100 | 0.172 | **0.257** | 0.415 |
| 1,000 | 0.241 | **0.327** | 0.415 |
| 10,000 | 0.248 | **0.327** | 0.415 |

### S1.2.1 Landfill emissions

We assume that carbon escapes from landfills as either $CO_2$ or $CH_4$. Given the paucity of data on PE degradation in landfills, we are unable to establish the ratio of carbon degradation products specific to PE. Thus, we assume emissions profiles consistent with landfill gas more generally. In the absence of methane management infrastructure such as methane flaring or energy production from landfill gas (LFG), we assume that 50% of carbon is released as $CO_2$ while 50% is released as $CH_4$.[12] This is a simplifying assumption because a fraction (up to 10%) of $CH_4$ will oxidize into $CO_2$ upon exiting the landfill. We do not account for that fraction. In the case of flaring or energy production from LFG, we assume that 75% of methane is oxidized via combustion.[12] The resulting fraction of carbon emissions in this case is 87.5% $CO_2$ compared to 12.5% emitted as $CH_4$. $CH_4$ emission are multiplied by their 100-year global warming potential (GWP) of 28, irrespective of when the emissions occur.[13] This amplifies the impact of $CH_4$ emissions when considering only a 100-year timeframe.[14] In the main body of our analysis, we report only the landfill case with flaring.

<u>The fraction of total polyethylene carbon released as $CO_2$ emissions from polyethylene and landfills at any time *t*:</u>

Fraction of polyethylene carbon released from energy combustion at time *t:*

Eq. 9

$$C_{energy}(t) = \sum_{i=1}^{t} 0.16 PE_W(i)$$

Fraction of polyethylene carbon released from landfill at time *t:*

Eq. 10

$$C_{LF}(t) = (1 - PE_{seq}) - C_{energy}(t)$$

At a landfill that flares 75% of methane into $CO_2$ the fraction of total C emissions that become $CO_2$ at time *t*:

Eq. 11

$$C_{CO2,\,flare}(t) = C_{energy}(t) + 0.875C_{LF}(t)$$

At a landfill that does not flare methane into $CO_2$ the fraction of total C emissions that become $CO_2$ at time *t*:

Eq. 12

$$C_{CO2,\,no-flare}(t) = C_{energy}(t) + 0.50C_{LF}(t)$$

The fraction of total polyethylene carbon released as $CH_4$ emissions from landfills at any time *t*:

At a landfill that flares 75% of methane into $CO_2$ the fraction of total C emissions that become $CH_4$ at time *t*:

Eq. 13

$$C_{CH4,\,flare}(t) = 0.125C_{LF}(t)$$

At a landfill that does not flare methane into $CO_2$ the fraction of total C emissions that become $CO_2$ at time *t*:

Eq. 14

$$C_{CH4,\,no-flare}(t) = 0.50C_{LF}(t)$$

## S1.3 Oriented strand board

We model the sequestration of carbon in oriented strand board (OSB) as a multi-phase process, with a use phase and then an end-of-life phase that may involve recycling, secondary use, and a significant portion managed in landfills or open dumps. The optimistic, moderate, and pessimistic cases for sequestration of carbon in OSB are derived from Skog (2008) and Stewart and Nakamura (2012), combining half-life estimates for the useful life of wood construction materials in single, multi-family, and residential upkeep scenarios with half-life estimates for wood construction materials decaying landfills.[11,15] The optimistic case assumes a useful half-life of 115 years based on OSB utilization in single family home construction. The pessimistic case assumes a useful half-life of 30 years based on OSB utilization in residential upkeep. The moderate case assumes a useful half-life of 72 years based on an end-use weighted average of half-lives for single family, multi-family, and residential upkeep construction. The stock of

carbon remaining in OSB in use ($OSB_{UL}$) from a production pulse of OSB ($OSB_0$) is estimated by a first-order decay model of the form:

Eq. 15

$$OSB_{UL}(t) = OSB_0 e^{-rt}$$

Where *r* is the decay rate determined by the half-life and *t* is time.

As a pulse of OSB exits its use-life, our analysis assumes the two most common end-of-life scenarios in the U.S.—landfill and energy production. We assume 70% of OSB waste is landfilled and 30% combusted for energy, which is consistent with estimates for California[15] and similar to national estimates in the literature.[11] Combusted OSB is assumed to release all of its carbon as $CO_2$.

In our analysis, we use a first-order exponential decay model with a decay rate based on landfill half-lives of 35, 29, and 20 years, for the optimistic, moderate, and pessimistic cases.[11,16] We assume that in the moderate case no more than 23% of the carbon in OSB in landfills is subject to decay, with lower and upper bounds at 1.3% and 34.6%.[11] The large recalcitrant fraction of OSB carbon is due in part to the recalcitrance of the lignin in wood products. Moreover, biological degradation rates are impacted by changes in chemical and environmental conditions (moisture, pH, oxygen) in landfill soils over time. For a more complete treatment of these topics, see Skog (2008).[11]

We then calculate the quantity of carbon remaining sequestered in OSB in-use or in landfills at any time *t* = 1 to 10,000 years (shown in **Fig. S1c**) where:

<u>The proportion of OSB carbon in use-life at any time *t*:</u>

If $OSB_{UL}(0) = 1$ then $OSB_{UL}(t)$ is calculated as:

Eq. 16

$$OSB_{UL}(t) = OSB_{UL}(0) e^{ut}$$

Where *u* is the use-life decay and *t* is time.

<u>The pulse of OSB carbon exiting use-life at any time *t*:</u>

Eq. 17

$$OSB_W(t) = OSB_{UL}(t-1) - OSB_{UL}(t)$$

<u>And entering landfills:</u>

Eq. 18

$$OSB_{New}(t) = 0.70 OSB_W(t)$$

The carbon remaining sequestered in the landfills at any time *t:*

Eq. 19

$$OSB_{LF}(t) = \sum_{i=1}^{t} f_{labile} OSB_{New}(i) e^{r(t-i)} + f_{recalc} OSB_{New}(i)$$

where *r* is the exponential decay rate of the OSB in landfills, and $f_{labile}$ and $f_{recalc}$ represent the labile and recalcitrant fractions of carbon, respectively.

Total carbon remaining sequestered at any time *t:*

Total carbon remaining sequestered is the sum of the fraction of carbon remaining in its useful life and the fraction remaining sequestered in the landfill.

Eq. 20

$$OSB_{seq}(t) = OSB_{UL}(t) + OSB_{LF}(t)$$

The fraction of carbon remaining in polyethylene and landfills at time t is shown in **Fig. S1c**. The estimated carbon loss to the atmosphere in each case is shown in **Table S4**.

**Table S4** -Percentage of OSB and landfill carbon loss to atmosphere over time. Values in bold-face reflect moderate assumptions used in the main text.

| Time since sequestration (years) | Carbon loss from OSB and landfills (%) - Optimistic | Carbon loss from OSB and landfills (%) - Moderate | Carbon loss from OSB and landfills (%) - Pessimistic |
|---|---|---|---|
| 100 | 0.135 | **0.249** | 0.441 |
| 1,000 | 0.304 | **0.456** | 0.532 |
| 10,000 | 0.305 | **0.456** | 0.532 |

### S1.3.1 Landfills

The assumptions for the fate of carbon in landfills are same as in the PE case. See **S.I. 1.2.1** for more details.

The fraction of total OSB carbon released as $CO_2$ emissions from OSB and landfills at any time *t*:

Fraction of OSB carbon released from energy combustion at time *t:*

Eq. 21

$$C_{energy}(t) = \sum_{i=1}^{t} 0.30 OSB_{W}(i)$$

Fraction of OSB carbon released from landfill at time *t:*

Eq. 22

$$C_{LF}(t) = (1 - OSB_{seq}) - C_{energy}(t)$$

At a landfill that flares 75% of methane into $CO_2$ the fraction of total C emissions that become $CO_2$ at time *t*:

Eq. 23

$$C_{CO2,\,flare}(t) = C_{energy}(t) + 0.875C_{LF}(t)$$

At a landfill that does not flare methane into $CO_2$ the fraction of total C emissions that become $CO_2$ at time *t*:

Eq. 24

$$C_{CO2,\,no-flare}(t) = C_{energy}(t) + 0.50C_{LF}(t)$$

The fraction of total OSB carbon released as $CH_4$ emissions from landfills at any time *t*:

At a landfill that flares 75% of methane into $CO_2$ the fraction of total C emissions that become $CH_4$ at time *t*:

Eq. 25

$$C_{CH4,\,flare}(t) = 0.125C_{LF}(t)$$

At a landfill that does not flare methane into $CO_2$ the fraction of total C emissions that become $CO_2$ at time *t*:

Eq. 26

$$C_{CH4,\,no-flare}(t) = 0.50C_{LF}(t)$$

## S1.4 Biochar

Our analysis assumes that biochar is produced as an agricultural soil amendment. Physical characteristics of the biochar (e.g. the O:C and H:C ratios) as well as environmental factors such as precipitation and soil conditions influence biochar stability; as such, there is a large degree of uncertainty in the durability of sequestration.[17–19] However, we have constrained our analysis to biochar manufactured for carbon storage purposes, and thus we set bounds on the quality of the biochar and the application conditions. These imposed constraints limit the fraction of labile carbon in the biochar. We calculate carbon sequestered in biochar in soils over 10,000 years using a two-pool model, representing the differing degradation rates of the labile and recalcitrant carbon fractions in the biochar. The carbon remaining in soils over time *t* is calculated with a double first-order exponential decay function of the form:

Eq. 27

$$C_{soil}(t) = C_{labile}e^{-r_{labile}t} + C_{recalc}e^{-r_{recalc}t}$$

Where $C_{soil}$ is the fraction of the original carbon pulse sequestered in biochar in soils, $C_{labile}$ is the labile fraction, $C_{recalc}$ is the recalcitrant fraction and $r_{labile}$ and $r_{recalc}$ are the decay constants of the fast and slow decaying biochar pools. The moderate case labile and recalcitrant fractions are assumed to be 3% and 97%, respectively, as treated in Wang, Xiong, and Kuzyiakov (2016).[20] For the optimistic case, we place a lower limit of 0.5% on the labile fraction. For the pessimistic case, the labile fraction is two standard deviations larger than the moderate case (~12%) based on the standard error reported in the source publication. The values for $r_{labile}$ and $r_{recalc}$ are taken from Santos, Torn, and Bird (2012), with the optimistic case estimates derived from andesite soils (table 3 in the referenced publication) minus two standard deviations.[21] The pessimistic case values are derived from the granite soil estimates plus two standard deviations. Decay rates for the fast (labile) and slow pools for each scenario are shown in **Table S5**. The moderate case values are the average of the unadjusted andesite and granite soil values. The estimated carbon remaining sequestered in biochar over 10,000 years is shown in **Fig. S1d**. The estimated cumulative fraction of biochar carbon returning to the atmosphere is shown in **Table S6**.

**Table S5** - Labile and recalcitrant pool decay rates for three scenarios

| | **Optimistic** | **Moderate** | **Pessimistic** |
|---|---|---|---|
| $\mathbf{r_{labile}}$ | 1.97 | 18.51 | 35.04 |
| $\mathbf{r_{recalc}}$ | 4.45e-4 | 3.40e-3 | 6.35e-3 |

**Table S6** - Percentage of biochar soil carbon leakage over time. Values in bold-face reflect moderate case assumptions used in the main text.

| **Time since sequestration (years)** | **Optimistic** | **Moderate** | **Pessimistic** |
|---|---|---|---|
| 100 | 0.048 | **0.31** | 0.56 |
| 1,000 | 0.36 | **0.97** | ~1.0 |
| 10,000 | 0.99 | **~1.0** | 1.0 |

## S2 Four biomass conversion pathways and life cycle emissions

This analysis is intended to highlight opportunities for carbon drawdown within a broad bioeconomy. The four selected pathways are not exhaustive, nor should the analysis be

interpreted as prescriptive. There are numerous economic, social, and ecological considerations that are not captured in a calculation of life cycle greenhouse gas emissions. We selected four pathways to represent a variety of conversion technologies and potential feedstocks. The selected pathways were deemed technically viable in the near-term, meaning that literature review and the authors' judgement selected for pathways that are presently commercial, in the demonstration phase, or have a combination of process components that have demonstrated technical viability.

Some components of the life cycle analysis (e.g. electric grid emissions) are regionally specific to California. This is due in part to existing policy support, commitment to decarbonization, and the state's willingness to be a test bed for innovative climate policy, such as the low-carbon fuel standard (LCFS). California also boasts significant biomass resources from its forestry, agricultural, and waste management sectors. Where possible, we rely on life cycle emissions estimates from Argonne National Laboratory's Greenhouse Gases, Regulated Emissions, and Energy Use in Transportation (GREET) model.[13] A variant of this model is used by participants in California's LCFS program to assess the carbon intensity of fuel pathways.

## S2.1 Notes on methodology

### S2.1.1 Carbon accounting

GREET takes a net-zero approach to biogenic carbon, i.e. when $CO_2$ is emitted from a biogenic source in a combustion process GREET accounts an equal offsetting biogenic credit. This is commensurate with the IPCC GHG national accounting methodology which takes a stock-change approach whereby emissions from biomass are assumed to occur at the point of harvest.[22] Hence, biogenic emissions from combustion or decay in later stages in the life cycle are assumed to be zero. This avoids double-counting in some policy contexts. However, this method ignores the climate impacts of biogenic carbon emissions from feedstocks with long regrowth cycles ("carbon debt"[23]), and it offers no way to credit the stocks of sequestered carbon in durable goods, landfills, and soil amendments.[24] Thus, we present results in two different ways. Our tabular results are presented the way GREET calculates emissions while our figures take a "flow-based" approach whereby carbon uptake is tracked from photosynthesis to final emission or storage. We maintain the tabular data consistent with GREET's methodology for cross-comparability.

For simplicity, we apply 100-year global warming potentials (GWP) to all GHG emissions, regardless of when they occur in time. This decision amplifies the relative climate impact of emissions that occur late in a project's lifetime (e.g. landfill emissions) when considering the 100-year time horizon, causing the estimates of net carbon removal presented here to be conservative within the GWP framework.[14] Dynamic life cycle assessment methods[14,24] can be used to account for these temporal discrepancies, but for the illustrative purposes here, we focus on the physical carbon drawdown rather than assessing the benefits of delayed impacts over a

fixed time horizon. The temporal impact considerations are out-of-scope and would only serve to enhance the apparent climate benefits of pathways that delay release of stored carbon ($CO_2$ emissions occurring near year 100 would approach zero impact). This is a distraction from the nominal carbon removal estimate we are after.

## S2.2 Feedstock selection

### S2.2.1 Switchgrass

Switchgrass is a fast-growing perennial crop that can generate high yields in diverse environments, including marginal lands unsuitable for conventional agriculture.[25] This is especially beneficial since limited land resources and competition for food production are key challenges for scaling up biomass production for carbon drawdown.

### S2.2.2 Corn stover

Corn stover is a residual agricultural feedstock. Agricultural wastes/residues have the advantage of not requiring additional land for cultivation. Most of the resources have already been expended to produce the primary agricultural good. The wastes/residues would otherwise degrade in situ, releasing a significant portion of their carbon back into the atmosphere.

### S2.2.3 Forest residues

Residues consist of the unmerchantable wood left over from logging activities in managed forests. Transport of residues presents logistical challenges.[26] When it is not cost-effective to transport or utilize residues, they may be burned onsite or left to decompose.

## S2.3 Switchgrass to electricity with CCS

We analyze the "cradle-to-grave" life cycle of an integrated gasification combined cycle (IGCC) power plant using the energy crop switchgrass as fuel. Carbon capture is accomplished with pre-combustion (solvent) removal of $CO_2$ from the shifted syngas.

**Table S7** – IGCC data sources

| **Process** | **LCI Source** |
|---|---|
| IGCC process emissions | GREET.net 2018[13] |
| Feedstock supply and transport | GREET.net 2018 |
| Captured $CO_2$ emissions | (Calculated) Excel model based on GREET carbon balance |
| CCS technical requirements | Kanniche et al. (2010)[27] |
| CCS energy emissions | Reduction in plant efficiency. No additional. |

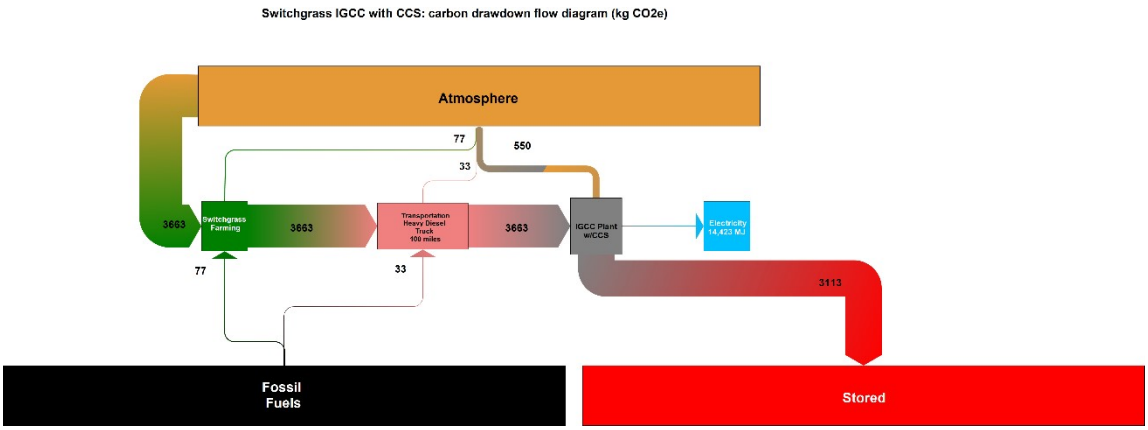


**Fig. S2** – Carbon flow through switchgrass IGCC system as $CO_2e$ per tonne of feedstock. Embodied fossil emissions as well as upstream fossil emissions associated with production inputs are included in the flow diagram at the point where those inputs enter the production process. Thus, fossil emissions exiting a box in the diagram include both onsite emissions and emissions associated with upstream production of inputs.

*Switchgrass Farming* – We assume switchgrass production takes place in California. There are suitable conditions for growing switchgrass throughout the state.[28] Farming emissions include nitrogen, nutrients, herbicides as well as diesel fuel and power for farming equipment. Electricity emissions are modeled using GREET's California distributed mix. Switchgrass travels 100 km by heavy diesel truck to the IGCC plant, under the assumption that the feedstock, IGCC power plant, and geological sequestration sites for $CO_2$ can be located proximately in California. We assume switchgrass feedstock is 46.6% elemental carbon by mass. This is equivalent to approximately 1,707 kg of potential atmospheric $CO_2$ per tonne of feedstock. Approximately 2.15 tonnes of feedstock are equivalent to the functional unit of 1 tonne C.

*IGCC Plant and Electricity Generation* – We assume the IGCC electric plant is also located in California, proximate (within 140 km) to depleted oil and gas reservoirs dispersed across the state where captured $CO_2$ might be sequestered. The feedstock functional unit of 1 tonne C (2.15 tonnes switchgrass) will yield 14,423 MJ of electricity under an assumption of 40% conversion efficiency, as modeled in GREET without carbon capture. Since this is the primary and only product from this process, we do not apply credits for displacement of grid electricity.

*Pre-combustion Carbon Capture and Compression* – We model pre-combustion capture of $CO_2$ after physical scrubbing with a methanol-based system as described in an analysis of a coal slurry IGCC system.[27] CSS system operation causes a 22% relative drop in plant efficiency in order to achieve an 85% capture rate. Earlier analyses of suboptimal bio-based IGCC reported capture efficiencies of around 50% at plant thermal efficiencies as low as 28%. [29] However, we assume the coal case to be closer to approximating what is possible in a modern optimized biomass IGCC facility with greater heat integration. The relative drop in plant efficiency reduces the overall thermal conversion efficiency of the plant from 40% to 31.2%. As a result, after scrubbing, capturing, and compressing process emissions, the output of the plant is reduced from 14,423MJ/tC to 11,250 MJ/tC in switchgrass.

*Land-use change* – GREET does not explicitly model land use change impacts for switchgrass or other dedicated energy crops used for electricity production. No credit or penalty is assigned in our analysis for this pathway.

### S2.3.1 Switchgrass to electricity results

**Table S8** shows the cradle-to-grave life cycle $CO_2$ emissions for switchgrass-IGCC without the benefit of CCS. The raw process emissions from electricity production are 3,772 kg $CO_2$/tC. However, 3,664 kg of that total are biogenic in nature and do not represent a positive emission to the atmosphere. Prior to CCS, the process yields net positive emission of 108 kg $CO_2$/tC, primarily resulting from feedstock production and transportation.

**Table S8** - Life cycle $CO_2$ emissions for switchgrass to electricity (kg$CO_2$/tC). Where "Process Emissions" are indicated, this includes emissions occurring onsite at the farm or facility such as stack emissions or nitrogen cycling in the field. "Upstream Emissions" include everything else, e.g. emissions from electric grid, embodied emissions in chemical inputs, extraction and refining emissions associated with fuels.

| **Life cycle emissions per 1 tonne C in feedstock** | | |
|---|---|---|
| **Products** | | |
| Electricity to grid (w/o CCS) | 14422.96 | MJ |
| **$CO_2$ Emissions** | | |
| Process Emissions (Switchgrass Farming) | 24.96 | kg |
| Process Emissions (IGCC) | 3661.87 | kg |
| Upstream Emissions (Switchgrass Farming) | 51.78 | kg |
| Transport Emissions (Farm to Plant) | 33.38 | kg |
| **Total Emissions** | **3771.99** | **kg** |
| Biogenic Credit (IGCC) | -3663.51 | kg |
| Biogenic Credit (Switchgrass Farming) | -0.05 | kg |
| **Lifecycle $CO_2$ (w/o CCS)** | **108.43** | **kg** |

We estimate 3,112 kg$CO_2$/tC (see **Table S9**) is captured from syngas clean-up by the CCS system. Electricity required to compress and pump the captured $CO_2$ to nearby geological sequestration sites is generated on-site. These emissions are already accounted for in the production process. As mentioned previously, the parasitic load for CCS results in a 3,173 MJ reduction in electricity generation. The final life cycle $CO_2$ emissions total -3,004 kg $CO_2$/tC once adjustments are made to reflect the CCS credit.

**Table S9** - Life cycle $CO_2$ adjustment for switchgrass IGCC pre-combustion CCS (per t C)

| **Life cycle emissions per 1 tonne C in feedstock** | | |
|---|---|---|
| | | |
| Captured $CO_2$ Credit | -3112.59 | kg |
| **Power Plant Efficiency Losses** | | |
| Carbon Capture Process Energy | 3173.05 | MJ |
| **Final Electricity to Grid** | **11249.91** | MJ |

| | | |
|---|---|---|
| **Life Cycle $CO_2$ (w/ capture)** | **-3004.17** | **kg** |

The final greenhouse gas potential is reflected in **Table S10.** Methane and nitrous oxide emissions are multiplied by their 100-year emissions factor to calculate the carbon dioxide equivalent ($CO_2e$) impact on climate. Nitrous oxide makes up the largest portion of this non-$CO_2$ impact, somewhat evenly distributed between the switchgrass cultivation process and the combustion at the IGCC plant. The additional 193 $kgCO_2e/tC$ from these emissions bring the total GHG impact of the bioelectricity process to -2,811 $kgCO_2e/tC$.

3,124 kWh (11,249 MJ)

**Table S10** - Non-GHG Emissions for Electricity Production from Switchgrass (kg/tC)

| **Non-$CO_2$ GHG Emissions (GHG 100 CO2e)** | | |
|---|---|---|
| | | |
| $CH_4$ (Process) x 28 $CO_2e$ | 10.10 | kg |
| $N_20$ (Process) x 265 $CO_2e$ | 182.96 | kg |
| **Non-$CO_2$ GHGs (in $CO_2e$)** | **193.06** | **kg** |
| **Life Cycle $CO_2e$ (w/ capture)** | **-2811.10** | **kg** |

### S2.3.2 IGCC drawdown over 100; 1,000; and 10,000 years

Here we combine cradle-to-gate emissions for IGCC electricity production with the sequestration models described in S.I. 1.1 to estimate the long-term sequestration benefit of the conversion pathway. At $t = 0$, 849 kgC (3,113 $kgCO_2e$) is sequestered in geological storage. Per the decay function described in Eq. 1 and the durability percentages described in **Table S2**, the cumulative $CO_2e$ leaked at each time $t$ is shown in **Table S11**.

**Table S11** – IGCC $CO_2$ leaked from geological sequestration over time (representative case in bold)

| **Case** | **100 years (kg $CO_2e/t$)** | **1,000 years (kg $CO_2e/t$)** | **10,000 years (kg $CO_2e/t$)** |
|---|---|---|---|
| Onshore - optimistic | 0.56 | 5.67 | 56.33 |
| **Onshore - moderate** | **2.63** | **26.42** | **254.56** |
| Onshore - pessimistic | 9.14 | 91.05 | 800.10 |
| Offshore - optimistic | 0.15 | 1.51 | 15.03 |
| Offshore - moderate | 0.59 | 5.93 | 58.82 |
| Offshore - pessimistic | 2.00 | 20.13 | 195.74 |

The moderate onshore case is selected as the representative case in our analysis. The 10,000-year drawdown profile of the pathway is shown in **Fig. S3.** At 100; 1,000; and 10,000 years, 99.9%, 99% and 91% of the original drawdown benefit remain, respectively.

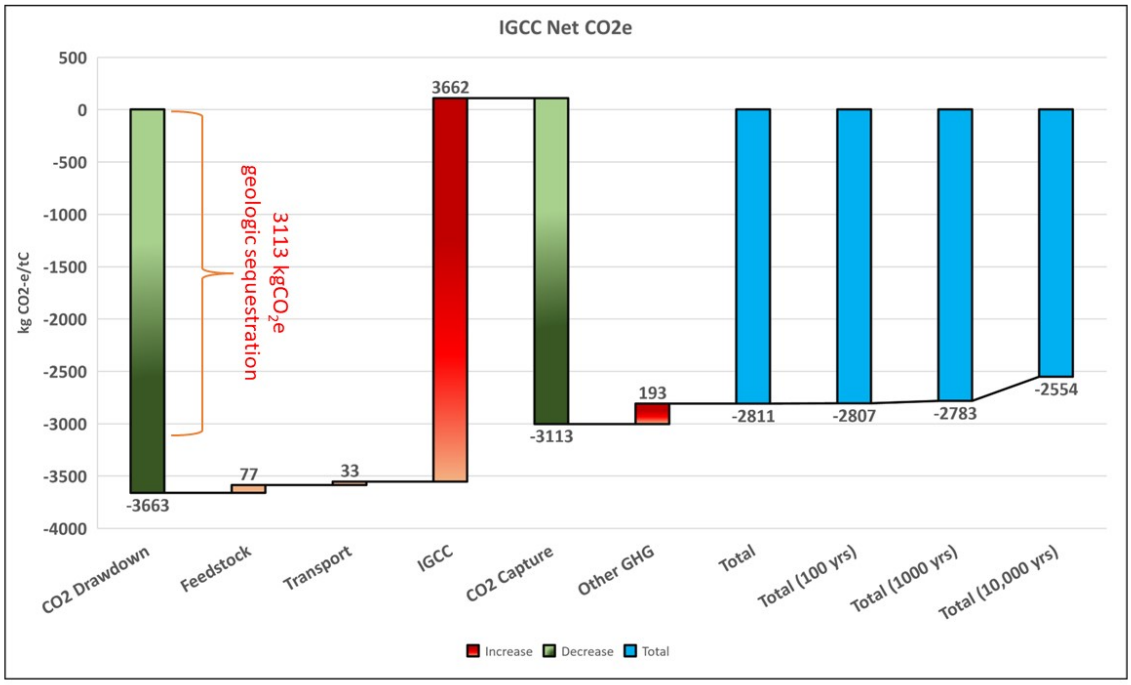


**Fig. S3** – IGCC-CCS electricity production from switchgrass - drawdown over 10,000 years (moderate case). Note that in the waterfall diagrams, green and red bars represent magnitudes of drawdown and emissions subsequent to the initial drawdown in biomass. The blue bars represent totals. The sum of all red and green bars is equal to the first blue bar.

## S2.4 Corn stover to polyethylene with CCS

We analyze the "cradle-to-grave" life cycle of a bio-polyethylene (PE) production supply chain based on lignocellulosic ethanol production from corn stover. Conversion of ethanol ($C_2H_5OH$) to bio-ethylene ($C_2H_4$) to polyethylene $(C_2H_4)_n$ is assumed to take place in the same refinery. The modeled facility integrates CCS to capture fermentation stage $CO_2$ during ethanol production.

**Table S12** – Polyethylene data sources

| **Process** | **LCI Source** |
|---|---|
| Feedstock handling and transport | GREET.net 2018[13] |
| Ethanol, Bio-ethylene, and polyethylene process emissions | GREET.net 2018 |
| Captured $CO_2$ emissions | (Calculated) Excel model based on GREET carbon balance |
| CCS technical requirements | NETL[30] |
| CCS energy emissions | GREET – California distributed grid mix |

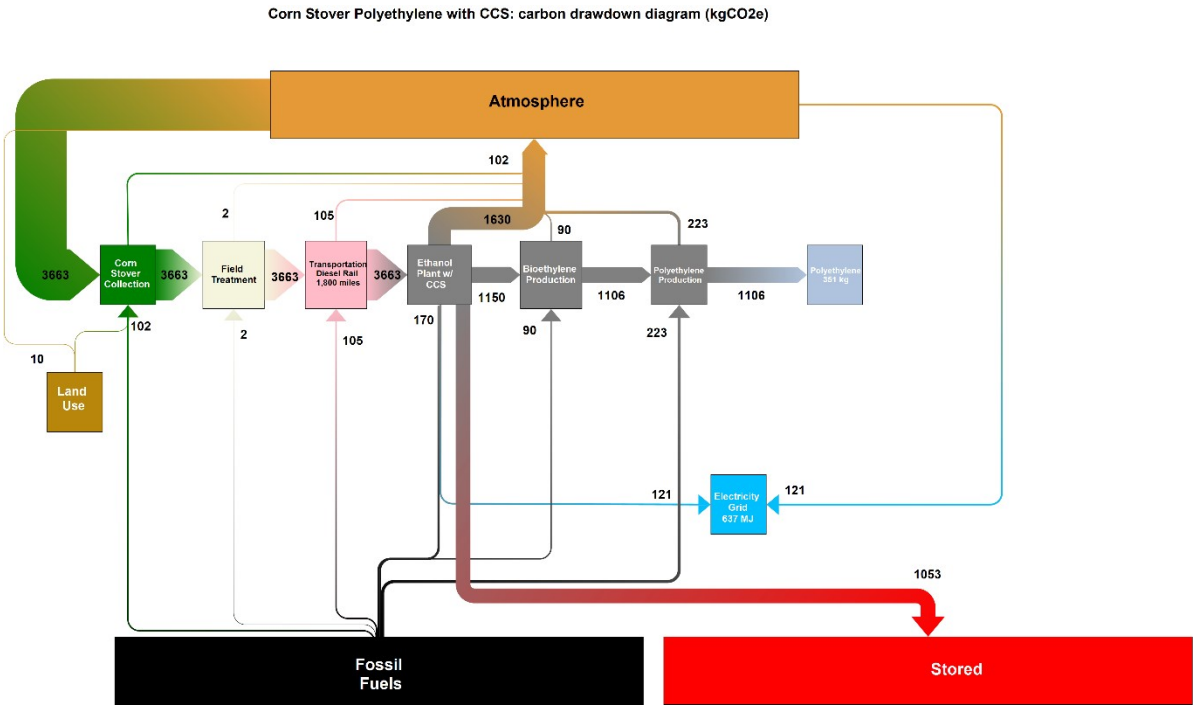


**Fig. S4** – Carbon flow through corn stover to polyethylene system with CCS as $CO_2e$ per tonne of feedstock. Embodied fossil emissions as well as upstream fossil emissions associated with production inputs are included in the flow diagram at the point where those inputs enter the production process. Thus, fossil emissions exiting a box in the diagram include both onsite emissions and emissions associated with upstream production of inputs. This diagram only shows the life cycle up to the point of resin production. Fabrication into finished products and the impact on the overall carbon intenisty of the process are discussed and calculate*d* below.

*Corn stover collection and field treatment* – Collection and treatment of corn stover is assumed to take place in Iowa, utilizing the GREET average U.S. Central and Southern Plains electric grid mix and associated transmission and distribution losses. Stover feedstock is assumed to travel 1,800 miles by diesel rail from farm to the refinery in California. Corn stover is assumed to be 46.6% elemental carbon by mass. This is equivalent to approximately 1,707 kg of potential atmospheric $CO_2$ per tonne feedstock. Approximately 2.15 tonnes of feedstock are equivalent to the functional unit of 1 tonne C.

*Ethanol production from corn stover* – The modeled refinery is assumed to be co-located with Bio-ethylene and PE upgrading facilities. We assume the facility is located near Fresno County, which is the approximate location of existing ethanol refineries. This location is also proximate to nearby oil and gas fields, which we are assuming would be amenable to geological sequestration. We are unaware of existing refineries in this region that convert lignocellulosic biomass to polyethylene, but this seems a suitable a location was such a facility to exist. Using GREET model yields, 1 ton of stover feedstock is equivalent to 280 kg (93 gal) of ethanol (EtOH) intermediate.

*Co-production of process and grid electricity from biomass* – Other than a small amount of energy from diesel—about 180 btu/gal EtOH—all process energy for the conversion of stover to

ethanol is assumed to come from combustion of a fraction of the stover feedstock to supply boiler heat and power generation. Approximately 400 kg/t of stover (858 kg/tC) is combusted on-site to deliver process heat and to generate power. The ethanol refinery is assumed to generate 814 MJ (1,746 MJ/tC) of electricity in excess of facility requirements. However, the excess is reduced to 637 MJ (1,366 MJ/tC) to account for the demands of capture and compression of $CO_2$, discussed in the subsequent sections. This remaining excess generation is exported to the grid and credits the life cycle carbon intensity of the plant by displacing an equivalent amount electricity from the average California grid.

*Carbon dioxide emissions from fermentation* - Carbon dioxide emissions are assumed to be internally consistent with the carbon content assumptions of resources and products employed by the GREET model. We assume that 46.6% of the mass of corn stover feedstock is carbon and 52.2% of the mass of the ethanol product is carbon. Approximately 40% of the stover is combusted for energy onsite. By mass-balance in Eq. 28, we obtain a fermentation emissions rate of 491 $kgCO_2e$/t of stover (or 1,053 $kgCO_2e$/tC).

Eq. 28

$$(0.466 \times 1000kg\ Stover) - (0.522 \times 280kg\ EtOH) - (0.466 \times 400kg\ Stover) \approx 134kg\ Carbon\ \#$$

$$134kg\ C \times \frac{44kgCO_2}{12kgC} \approx 491kgCO_2$$

*Capture and compression of fermentation carbon dioxide* - We employ a simple model of fermentation $CO_2$ capture. Fermentation $CO_2$ streams are relatively pure, and we assume a 90% concentration coming from the fermentation vent.[30] Clean-up and capture of the $CO_2$ requires only dehydration and compression to a supercritical pipeline pressure. We assume a 100% capture rate and calculate the energy demand and associated emissions of a five stage $CO_2$ compressor with a suction pressure of 17.4 psia at 81° F. [30] Assuming a pressure drop of 35 kPa/km (5.07 psia/km) and a minimum outlet pressure of 10.3 MPa (1494 psia) [31] and excluding elevation, this pressure is sufficient to pump compressed $CO_2$ roughly 140 km**.** The energetic cost of this process is estimated to be 100.09 kWh/t $CO_2$ captured.[30] Electricity for capture and compression is modeled as a reduction in excess co-product electricity. The energy requirement to capture fermentation $CO_2$ is approximately 49 kWh/t of stover processed as shown in Eq. 29.

Eq. 29

$$(0.10009kWh)/kgCO_2 \times 490kgCO_2/t\ Stover \approx 49.1\ kWh/t\ stover$$

*Land use change*— GREET's assumptions for land use change (LUC) account for both direct (domestic) and indirect (international) land use change using the CCLUB model. Land use change scenarios from biofuels production are modeled using Purdue University's Global Trade Analysis Project (GTAP) model, which is a computable general equilibrium model. GTAP determines potential land use changes domestically and internationally contingent on a set of biomass-to-ethanol production scenarios. This analysis utilizes the Stover Ethanol scenario and associated LUC elasticities. This scenario assumes a growth in corn ethanol production from 3.41 billion gallons (BG) to 15 BG and an additional 9 BG of ethanol from stover between 2004 and 2034, which is the end of the recommended 30-year production horizon in the CCLUB

model. This expansion of ethanol is also consistent with U.S. Department of Energy [32] Billion-Ton Report assumptions. Domestic emissions are modeled using the CENTURY model while international emissions are modeled using the Winrock model. The LUC emissions amortization period is set equivalent with the production period at 30 years. The model considers 100 cm soil depth for soil organic carbon (SOC) calculations, and it is assumed that, internationally, biomass is burned to clear land. Within the CENTURY model, tilling practices are set as the U.S. average, and the yield scenario assumes a 1% increasing annual yield. Where the model predicts forest conversion to cropland, the model settings adopt a Harvested Wood Products (HWP) assumption from Heath *et al.* [33]. This setting assumes that 60% of converted forest live and dead wood will be harvested. 21% of the harvested portion will end up in durable wood products. 21% will be burned for energy. 18% will be released as $CO_2$ to the atmosphere. The remaining 40% of waste wood will also be released to the atmosphere. Notably, the stover scenario results in net carbon sequestration even though there is equivalent corn ethanol production as in the corn ethanol scenario. This is because the "GTAP [model] predicts a small amount of gains in forest lands that result in carbon sequestration, offsetting carbon emissions from limited conversion of cropland pasture to corn agriculture." [34]

*Ethanol conversion to Bio-ethylene and polyethylene*— Bio-ethylene and polyethylene production are assumed to be co-located with the ethanol refinery. However, natural gas and power are provided by conventional utilities rather than direct integration with the ethanol facility. The ethylene process consumes natural gas at a rate of 2,457 btu/kg of Bio-ethylene. Electricity consumption is 1,189 btu/kg of Bio-ethylene. Electricity use is modeled as distributed from the average California grid mix. Similarly, Bio-ethylene conversion to polyethylene requires natural gas, electricity, residual oil, and liquified petroleum gas combustion onsite. The energy consumption rates are 7.230 btu/kg, 2,005 btu/kg, 55.11 btu/kg, and 0.90 btu/kg of polyethylene produced, respectively. The yield ratios from ethanol to ethylene to PE are approximately 1.71 **:** 1.01 **:** 1 on a mass basis. There is unreacted and recycled material in the ethanol to Bio-ethylene conversion process. This results in roughly 9.3 kg of carbon (34 kg$CO_2$e) exiting the mass balance of the process. Some of this material would be recycled, but for simplicity, we chose to track this material but not update the feedstock requirements.

*Upgrading polyethylene to products*

This cradle-to-gate assessment is intended to represent a general polyethylene resin production process. There are many varieties and end-uses of polyethylene (e.g. LDPE, HDPE, LLDPE). After production of the PE resin, further life cycle steps will be undertaken to transform PE resin to end-products. Potential processes include the production of films, injection molding, compression molding, and extrusion. All these processes will incur additional process emissions. In the tabular data below, we exclude the final product phase. But for the representative case, we include additional emissions from injection molding. HDPE bottles we selected as the representative case for PE. Bottles are produced by blow molding, which is a form of injection molding whereby PE is heated and injected into a mold and then compressed air expansion is used to form a hollow receptacle. Emissions factors from GREET for compressions molding,

injection molding, and extrusion are shown in **Table S13**. We note that GREET's emissions estimates for injection molding are lower than other published LCAs.[35]

**Table S13** – Conversion of polyethylene resin to products process emissions

| | **Compression Mold (kg $CO_2$e/t feed)** | | | **Extrusion (kg $CO_2$e/t feed)** | | | **Injection Mold (kg $CO_2$e/t feed)** | | |
|---|---|---|---|---|---|---|---|---|---|
| | **$CO_2$** | **$CH_4$** | **$N_2O$** | **$CO_2$** | **$CH_4$** | **$N_2O$** | **$CO_2$** | **$CH_4$** | **$N_2O$** |
| **LDPE** | 158 | 7.56 | 0.64 | 29 | 2.26 | 0.17 | 150 | 8.2 | 0.6 |
| **HDPE** | 99 | 7.56 | 0.64 | 29 | 2.26 | 0.17 | 150 | 8.2 | 0.6 |

### S2.4.1 Corn Stover to Polyethylene Results

The stover to PE process with CCS yields a net drawdown of -1,595 kg $CO_2$e/tC. As illustrated in **Fig. S4**, photosynthetic drawdown for the feedstock stage is around 3,663 kg$CO_2$/tC. The polyethylene product stores 1,106 kg $CO_2$e of the biogenic carbon. Excess process electricity is provided to the grid, displacing alternative electricity generation. Capture of fermentation $CO_2$ further improves the performance of this process, bringing it well into the net negative emissions (drawdown) range.

Cradle-to-gate life cycle $CO_2$ emissions for stover polyethylene resin without the benefit of CCS are shown in **Table S14**. The product yield for polyethylene is 351 kg/tC. The process generates an excess 1,747 MJ/tC of electricity, but the parasitic load of the CCS system reduces excess generation to 1,367 MJ/tC. The process emissions from ethanol production are significant but since they originate from stover combustion, they do not contribute significantly to the carbon intensity of the process. The process is credited -121 kg$CO_2$e/tC for displacement of grid electricity, and land use further credits the process -10 kg$CO_2$e/tC, implying an increase in terrestrial carbon stocks (see Land Use section above for full explanation). Before accounting CCS removals, the process stands at a net negative emission of approximately -542 kg$CO_2$e/tC.

**Table S14** - Life cycle $CO_2$ emissions for polyethylene production from stover. Where "Process Emissions" are indicated, this includes emissions occurring onsite at the farm or facility such as stack emissions or nitrogen cycling in the field. "Upstream Emissions" include everything else, e.g. emissions from electric grid, embodied emissions in chemical inputs, extraction and refining emissions associated with fuels.

| **Life cycle outputs from 1 metric ton corn stover in GREET** | | |
|---|---|---|
| **Products** | | |
| Polyethylene | 350.80 | kg |
| Electricity to grid (Ethanol Stage) | 1366.95 | MJ |
| **$CO_2$ Emissions** | | |
| Process Emissions (Stover Collection at Farm) | 47.87 | kg |
| Upstream Emissions (Stover Collection at Farm) | 53.88 | kg |
| Process Emissions (TDCHS) | 0.00 | kg |

| | | |
|---|---|---|
| Upstream Emissions (TDCHS) | 1.66 | kg |
| Transport (stover) | 105.15 | kg |
| Process Emissions (Ethanol) | 2526.28 | kg |
| Upstream Emissions (Ethanol) | 169.60 | kg |
| Process Emissions (Bio-ethylene) | 51.60 | kg |
| Upstream Emissions (Bio-ethylene) | 38.39 | kg |
| Process Emissions (Polyethylene) | 153.17 | kg |
| Upstream Emissions (Polyethylene) | 69.62 | kg |
| Total Emissions | **3217.22** | **kg** |
| Displaced Electricity credit | -120.71 | kg |
| Total w/ Co-product credits | **3096.52** | kg |
| Biogenic Credit (Stover Collection) | -0.07 | kg |
| Biogenic Credit (Ethanol) | -2522.26 | kg |
| LUC | -10.10 | kg |
| (Direct) | -2.83 | kg |
| (Indirect) | -7.26 | kg |
| $CO_2$e Stored in Polyethylene Credit | -1106.16 | kg |
| "Cradle to Gate" $CO_2$ | **-542.07** | **kg** |

The representative case for polyethylene in our manuscript are HDPE bottles which require an additional fabrication step of injection molding. Emissions for this step derived from the "per tonne feedstock" values in **Table S13** and 2.15 tonnes of feedstock per functional unit of "1 tonne C in biomass." After fabrication, net process emissions are -201 $kgCO_2e/tC$

**Table S15** - Life cycle $CO_2$ emissions for fabrication of PE resin to bottles

| **Emissions associated with injection molding to bottles** | | |
|---|---|---|
| | | |
| $CO_2$ emissions | 322.00 | kg |
| Non-$CO_2$ GHGs (in $CO_2$e) | 19.00 | kg |
| **Life Cycle $CO_2$e after fabrication** | **-201.07** | **kg** |

Carbon captured from the fermentation stage of ethanol production is estimated to be 1,053 $kgCO_2/tC$, as shown in **Table S16**. Electricity required to compress and pump the captured $CO_2$ to nearby geological sequestration sites is generated on-site. These emissions are already accounted for in the production process emissions. The impact of the CCS system is a reduction of excess electricity provided to the grid. The parasitic load for CCS results in a 380 MJ reduction in electricity export. After CCS, life cycle GHG emissions total -1,254 $kgCO_2/tC$.

**Table S16** - Life cycle $CO_2$ adjustment for stover to polyethylene fermentation CCS

| **Life cycle emissions per 1 tonne C in feedstock** |
|---|

| | | |
|---|---|---|
| Captured $CO_2$ Credit | **-1053.34** | kg |
| Life Cycle $CO_2$ (w/ capture) | **-1254.41** | **kg** |

The final $CO_2e$ intensity is reflected in **Table S17**. Methane and nitrous oxide emissions from all processes (except injection molding, which are already accounted above) are multiplied by their 100-year emissions factor to calculate the carbon dioxide equivalent ($CO_2e$) impact on climate. Methane makes up the largest portion of this non-$CO_2$ impact, and those emissions primarily originate upstream from the stover collection process in the production of nitrogen fertilizer. The additional 58 $kgCO_2e/tC$ from these emissions bring the total cradle-to-gate emissions to -1,197 $kgCO_2e/tC$ before upgrading of PE to final product.

**Table S17** - Non-GHG Emissions for polyethylene production from corn stover

| **Non-$CO_2$ GHG Emissions and Total Life cycle $CO_2e$** | | |
|---|---|---|
| | | |
| $CH_4$ (Process) x 28 $CO_2e$ | 41.47 | kg |
| $N_20$ (Process) x 265 $CO_2e$ | 16.40 | kg |
| **Non-$CO_2$ GHGs (in $CO_2e$)** | **57.86** | **kg** |
| **Life Cycle $CO_2e$ (w/ capture)** | **-1196.55** | **kg** |

### S2.4.2 Polyethylene drawdown over 100; 1,000; and 10,000 years

Here we combine cradle-to-gate emissions for polyethylene production with the sequestration models described in S.I. 1 to estimate the long-term sequestration benefit of the conversion pathway. At $t = 0$, 302 kgC (1,106 kg $CO_2e$) is sequestered in the polyethylene product and 287 kgC (1,053 $kgCO_2e$) is sequestered in geological storage.

Per the decay function described in Eq. 1 and the sequestration percentages described in **Table S2**, the cumulative $CO_2e$ emitted at each time $t$ from geological sequestration is shown in **Table S18.**

**Table S18** – Polyethylene $CO_2$ emitted from geological sequestration over time (representative case in bold)

| **Case** | **100 years (kg $CO_2e$/t)** | **1,000 years (kg $CO_2e$/t)** | **10,000 years (kg $CO_2e$/t)** |
|---|---|---|---|
| Poly. (geologic onshore) optimistic | 0.19 | 1.94 | 19.26 |
| **Poly. (geologic onshore) moderate** | **0.90** | **9.03** | **87.04** |
| Poly. (geologic onshore) pessimistic | 3.13 | 31.13 | 273.55 |

The carbon remaining in the polyethylene at 100; 1,000; and 10,000 years is estimated according to the functions described by Eq. 3 through Eq. 8, The quantity of polyethylene carbon emitted at *t* is calculated by Eq. 9 and Eq. 10. The quantity of $CO_2$ and $CH_4$ emissions from energy production and landfill emissions at each time *t* is calculated by Eq. 11 and Eq. 13 in the case of a landfill that flares fugitive methane emissions.

**Table S19** – Flaring case landfill emissions (representative case in bold)

| Case | Emission | 100 years (kg $CO_2$e/tC) | 1,000 years (kg $CO_2$e/tC) | 10,000 years (kg $CO_2$e/tC) |
|---|---|---|---|---|
| Poly (product C) optimistic | $CO_2$ (energy) | 138.58 | 192.35 | 192.35 |
| | $CO_2$ (landfill) | 45.28 | 64.63 | 71.25 |
| | $CH_4$ (landfill) | 65.86 | 94.01 | 103.64 |
| **Poly (product C) moderate** | **$CO_2$ (energy)** | **192.35** | **192.35** | **192.35** |
| | **$CO_2$ (landfill)** | **80.07** | **148.54** | **148.54** |
| | **$CH_4$ (landfill)** | **116.47** | **216.05** | **216.05** |
| Poly (product C) pessimistic | $CO_2$ (energy) | 192.35 | 192.35 | 192.35 |
| | $CO_2$ (landfill) | 233.12 | 233.12 | 233.12 |
| | $CH_4$ (landfill) | 339.08 | 339.08 | 339.08 |

In the case of a landfill that does not flare fugitive landfill emissions, $CO_2$ and $CH_4$ are calculated by Eq. 12 and Eq. 14. In this case, $CH_4$ emissions are much greater.

**Table S20** – Non-flaring case landfill emissions (representative case in bold)

| Case | Emission | 100 years (kg $CO_2$e/tC) | 1,000 years (kg $CO_2$e/tC) | 10,000 years (kg $CO_2$e/tC) |
|---|---|---|---|---|
| Poly (product C) optimistic | $CO_2$ (energy) | 138.58 | 192.35 | 192.35 |
| | $CO_2$ (landfill) | 25.87 | 36.93 | 40.72 |
| | $CH_4$ (landfill) | 263.43 | 376.04 | 414.56 |
| **Poly (product C) moderate** | **$CO_2$ (energy)** | **192.35** | **192.35** | **192.35** |
| | **$CO_2$ (landfill)** | **45.76** | **84.88** | **84.88** |
| | **$CH_4$ (landfill)** | **465.89** | **864.22** | **864.22** |
| Poly (product C) pessimistic | $CO_2$ (energy) | 192.35 | 192.35 | 192.35 |
| | $CO_2$ (landfill) | 133.21 | 133.21 | 133.21 |
| | $CH_4$ (landfill) | 1356.32 | 1356.32 | 1356.32 |

The full emissions profile of corn stover to polyethylene bottles (moderate case), assuming that landfills combust or flare methane emissions, is shown in **Fig. S5**. This calculation also includes the additional fabrication emissions (341 kg $CO_2$e/tC) for injection molding shown in **Table S13**, bringing the cradle-to-gate emissions to -1,197 kg$CO_2$e/tC. At 100; 1,000; and 10,000 years, 67%, 53% and 46% of the original drawdown benefit remain, respectively.

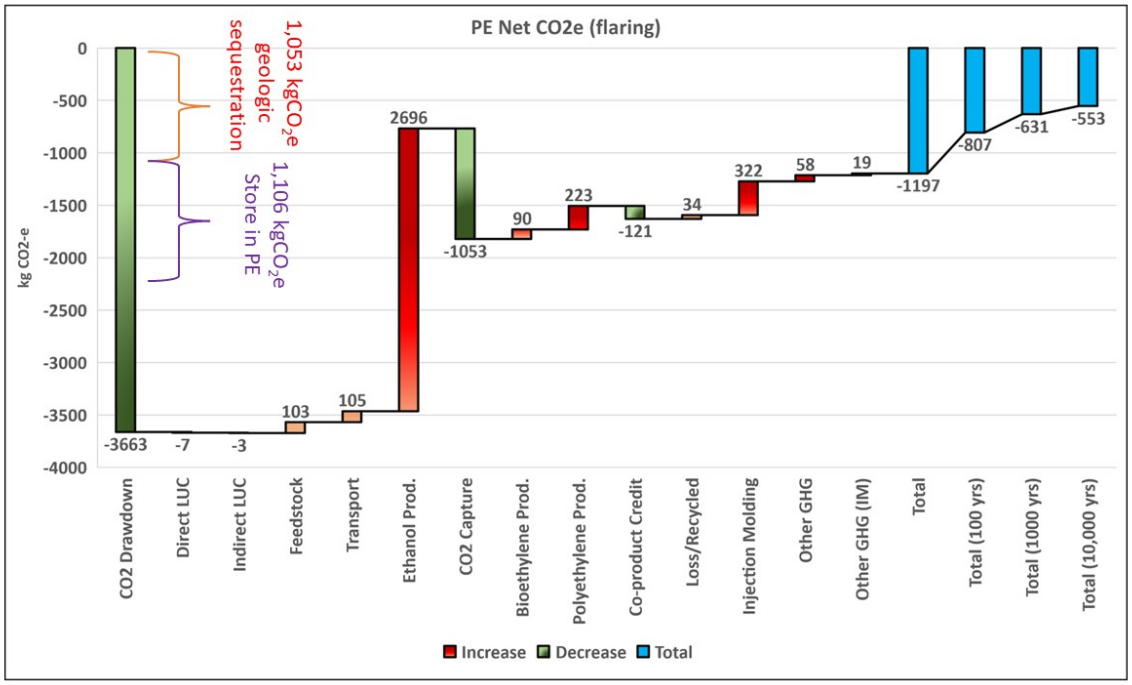


**Fig. S5** – Polyethylene with CCS drawdown over 10,000 years (moderate case/flared landfills). Note that in the waterfall diagrams, green and red bars represent magnitudes of drawdown and emissions subsequent to the initial drawdown in biomass. The blue bars represent totals. The sum of all red and green bars is equal to the first blue bar.

The full emissions profile of corn stover to polyethylene bottles (moderate case) assuming that landfills do not control methane emissions by flaring is shown in **Fig. S6**. This calculation also includes the additional fabrication emissions (341 kg $CO_2$e/tC) for injection molding shown in **Table S13,** bringing the cradle-to-gate emissions to -1,197 kg$CO_2$e/tC. At 100; 1,000; and 10,000 years, 41%, 4% and 0% of the original drawdown benefit remain, respectively. At the 10,000 years, the conversion process yields net emissions.

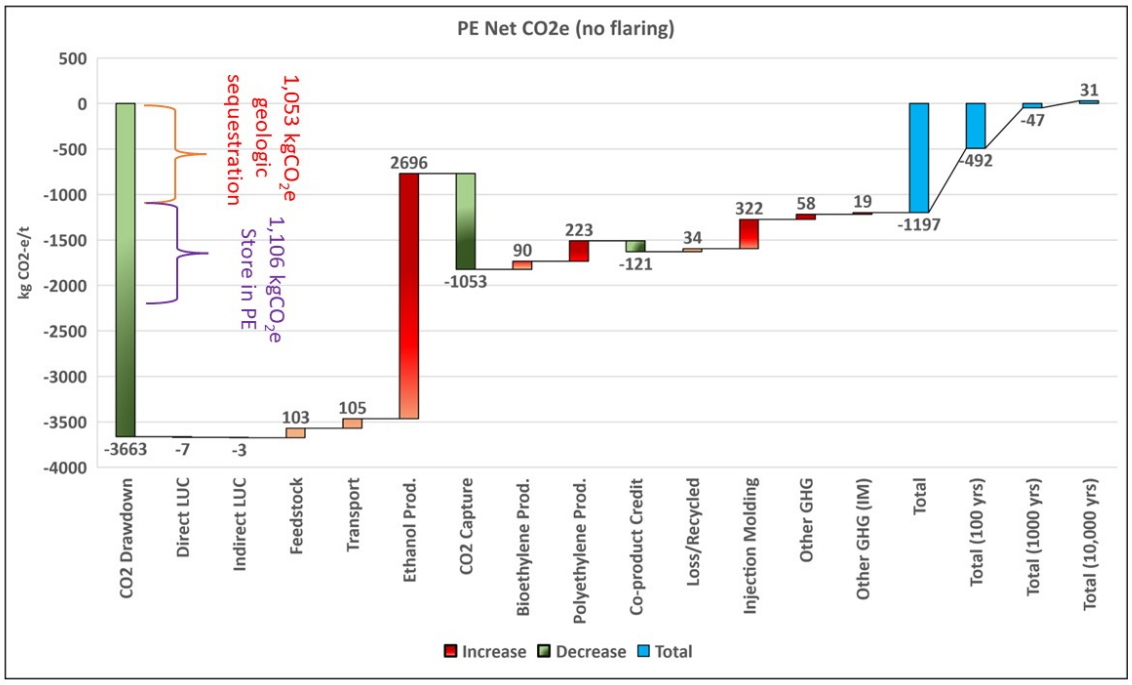


**Fig. S6** - Polyethylene with CCS drawdown over 10,000 years (moderate case/unflared landfills). Note that in the waterfall diagrams, green and red bars represent magnitudes of drawdown and emissions subsequent to the initial drawdown in biomass. The blue bars represent totals. The sum of all red and green bars is equal to the first blue bar.

## S2.5 Forest residues to biochar

We model the "cradle-to-grave" life cycle emissions of a commercial forest residue to biochar system incorporating an air curtain burner. Carbon sequestration is achieved through physical storage in the biochar product and subsequent agricultural soil amendment. We analyze a simple biochar process using an air curtain burner (ACB). An ACB is typically used for the complete combustion of biomass. However, operations can be modified to achieve "flame cap" pyrolysis, with slow pyrolysis taking place in the base of the firebox alongside complete combustion in the upper layer. The ACB can be set up at remote locations for the management of forest residues.

**Table S21** – Biochar data sources

| **Process** | **LCI Source** |
|---|---|
| Feedstock handling and transport | GREET.net 2018[13] |
| Gate-to-gate airburner yields and emissions | Puettmann (2017)[36] |
| Upstream energy and fuels | GREET.net 2018 |

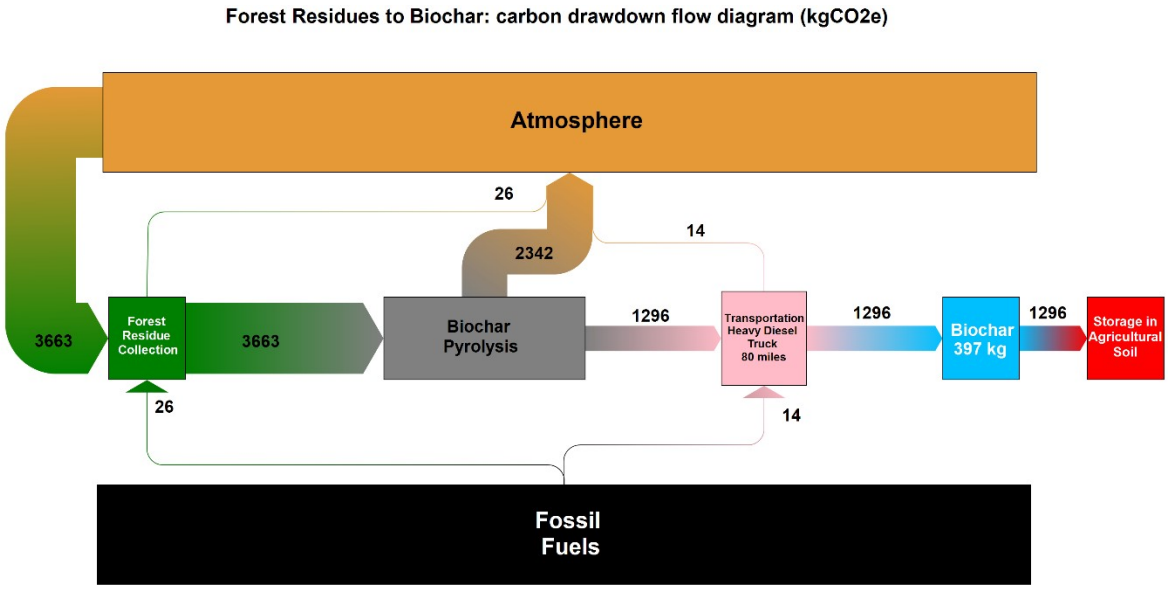


**Fig. S7** - Carbon flow through forest residues to biochar system as $CO_2e$ per tonne of feedstock. Note that carbon in methane and carbon monoxide emissions are not shown in this figure. These emissions account for the balance of carbon in the feedstock. Embodied fossil emissions as well as upstream fossil emissions associated with production inputs are included in the flow diagram at the point where those inputs enter the production process. Thus, fossil emissions exiting a box in the diagram include both onsite emissions and emissions associated with upstream production of inputs.

*Forest Residue Collection* – forest residue collection is assumed to take place in Northern California. The feedstock is co-located with the biochar process, as the ACB is designed to be mobile. The forest residue is assumed to be 50.3% carbon by mass which is equivalent to 1,844 kg of atmospheric $CO_2$/t of feedstock. Feedstock handling energy and emissions are taken from GREET. We note that the energy requirement assumptions for feedstock handling in GREET are substantially smaller than those reported in Puettmann (2017).[36] GREET assumes about 139 MJ (131,750 Btu) or approximately 4 L of diesel per ton of feedstock handled. While Puettmann assumes 2,300 MJ (2.18 MMBtu) or roughly 88 L of propane/LPG per ton of feedstock. We rely on the GREET estimate for consistency with our other pathways.

*Biochar Production via Pyrolysis* – The ACB is a relatively simple technology comprised of a refractory-lined box with a high-powered blower. The modeled process draws upon conversion efficiencies and GHG emission factors from Puettmann (2017).[36] The modeled process converts 5,000 kg (bone dry basis) of forest residue to 1,000 kg of biochar with carbon content of 89%. We modified the carbon mass-balance for consistency with GREET. The carbon balance in the source literature implies a forest residue carbon content of 39% or an unreported bio-oil or liquid VOC fraction. Assuming that in the latter case, bio-oil would be combusted in an air burner batch process, we adjust biochar conversion $CO_2$ emissions up from 0.78 kg/kg of forest residues to 1.18 kg/kg. This is consistent with a forest residue carbon content of 50.3% as in GREET and the OSB pathway we analyzed. For simplicity, non-$CO_2$ carbon emissions in the carbon balance ($CH_4$ & CO) as adapted from the reference literature are held constant.

*Biochar End-of-Life* – Produced biochar is assumed to be transported roughly 80 miles by truck from forest site to agricultural soils in the California Central Valley region.

### S2.5.1 Forest Residue to Biochar Results

The biochar technology in this analysis has potential as a negative emissions pathway at -963kg $CO_2$e/tC. Cradle-to-gate life cycle $CO_2$ emissions for forest residue to biochar are shown in **Table S22.** The biochar production yield is 397 kg/tC. Photosynthetic drawdown in the feedstock is 3,663 kg$CO_2$/tC of forest residue (see **Fig. S7**). The onsite and upstream process $CO_2$ emissions for biochar production total 2,343 kg $CO_2$/tC, all of which are biogenic. Carbon is physically stored (-1,296 kg$CO_2$e/tC) in agricultural soils. When considering only $CO_2$ emissions, the cradle-to-gate emissions are roughly -1,281 kg$CO_2$/tC.

**Table S22** - Life cycle $CO_2$ emissions for biochar production. Where "Process Emissions" are indicated, this includes emissions occurring onsite at the farm or facility such as stack emissions or nitrogen cycling in the field. "Upstream Emissions" include everything else, e.g. emissions from electric grid, embodied emissions in chemical inputs, extraction and refining emissions associated with fuels.

| **Life cycle emissions per 1 tonne C in feedstock** | | |
|---|---|---|
| **Products** | | |
| Biochar | 397 | kg |
| **$CO_2$ Emissions** | | |
| Process Emissions (Forest Residue Collection) | 22.43 | kg |
| Upstream Emissions (Forest Residue Collection) | 4.09 | kg |
| Process Emissions (Biochar Production) | **2342.41** | kg |
| Upstream Emissions (Biochar Production) | 0.00 | kg |
| Transport Biochar to Farm | 14.44 | kg |
| Total Emissions | **2383.37** | **kg** |
| Biogenic Credit (Biochar Production) | -2342.41 | kg |
| Biogenic Credit (To balance non-$CO_2$ emissions) | -25.81 | kg |
| $CO_2$ Stored in Biochar Credit | -1295.73 | kg |
| "Cradle to Gate" $CO_2$ | **-1280.58** | **kg** |

However, the non-$CO_2$ GHG emissions have a significant impact on the final emissions intensity. The combined effect of methane (~145 kg$CO_2$e/tC) and $N_2O$ (~173 kg$CO_2$e/tC) bring the cradle-to-gate emissions to -963 kg$CO_2$e/tC, as shown in Table S23.

**Table S23** - Non-GHG emissions for biochar production

| **Non-$CO_2$ GHG emissions (GHG 100 CO2e) and total life cycle $CO_2$e** | | |
|---|---|---|
| | | |
| $CH_4$ (Process) x 28 CO2e | 145.42 | kg |
| $N_20$ (Process) x 265 CO2e | 172.56 | kg |
| **Non-$CO_2$ GHGs (in $CO_2$e)** | **317.98** | **kg** |

| Life cycle $CO_2e$ | -962.59 | kg |
|---|---|---|

**Fig. S7** shows sources and sinks of emissions in the biochar process. Emissions contributions are largely biogenic from the pyrolysis process. About 35% of available biogenic carbon is stored in the biochar. Non-$CO_2$ GHG emissions represent 12% of total emissions when biogenic $CO_2$ is included. Non-$CO_2$ GHG's are almost eight times greater than fossil $CO_2$ emissions.

### S2.5.2 Biochar drawdown over 100; 1,000; and 10,000 years

Here we combine cradle-to-gate emissions for forest residues converted to a biochar soil amendment with the sequestration models described in S.I. 1 to estimate the long-term sequestration benefit of the conversion pathway. At $t = 0$, 353 kgC (1,296 kg$CO_2$e/tC) is sequestered in the biochar in soils. Per the decay function described in Eq. 27 and the sequestration losses described in **Table S6,** the cumulative $CO_2$e emitted at each time $t$ is shown in **Table S24**.

**Table S24** – Biochar $CO_2$ emitted from soil sequestration over time (representative case in bold)

| **Case** | **100 years (kg $CO_2$e/tC)** | **1,000 years (kg $CO_2$e/tC)** | **10,000 years (kg $CO_2$e/tC)** |
|---|---|---|---|
| Biochar - optimistic | 62.09 | 469.46 | 1280.72 |
| **Biochar - moderate** | **397.95** | **1253.58** | **1295.73** |
| Biochar - pessimistic | 719.34 | 1293.83 | 1295.73 |

The moderate case is selected as the representative case. The 10,000-year drawdown profile of the pathway is shown in **Fig. S8**. At 100 years, 59% of the original drawdown benefit remains. At 1,000 and 10,000 years, the process yields net positive emissions.

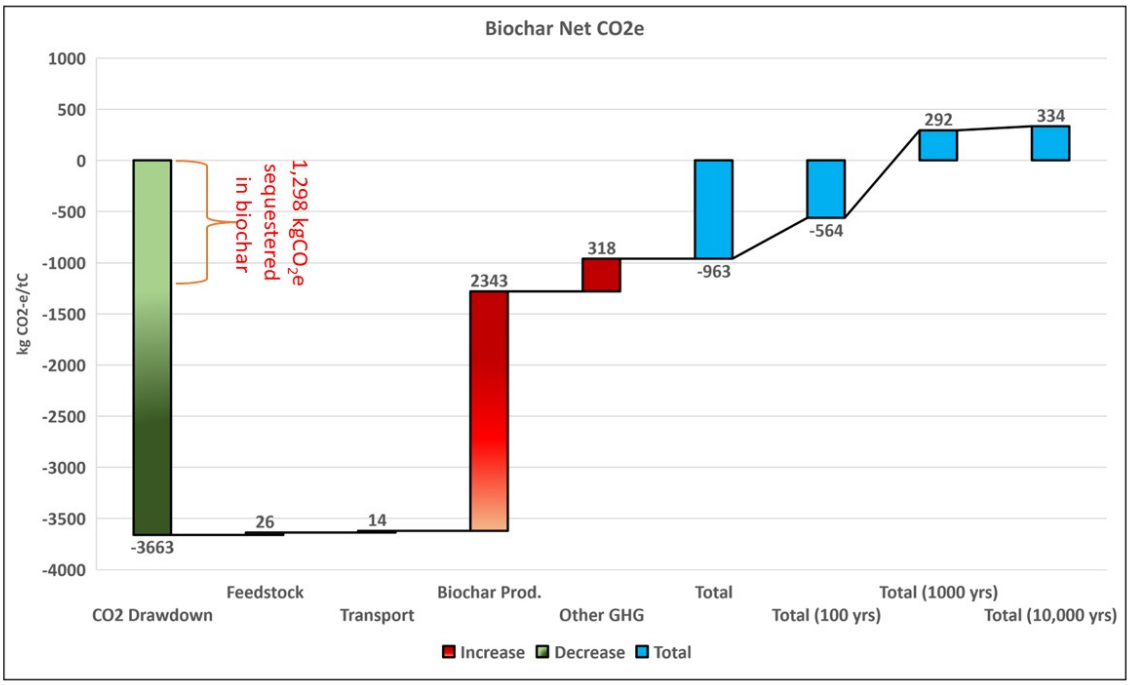


**Fig. S8** – Biochar soil amendment drawdown over 100 years (moderate case). Note that in the waterfall diagrams, green and red bars represent magnitudes of drawdown and emissions subsequent to the initial drawdown in biomass. The blue bars represent totals. The sum of all red and green bars is equal to the first blue bar.

## S2.6 Forest Residues to OSB

We analyze the "cradle-to-grave" life cycle of oriented strand board (OSB) construction material from forest residues. A standard production unit of OSB is measured at 1,000 $ft^2$ at 3/8" thickness. A tonne of forest residue feedstock will produce roughly 1.3 units with an estimated mass of 769 kg. To produced OSB, wood strands approximately 2.5 cm x 15 cm are layered at opposing angles and compressed under high temperatures with resin and wax (about 5% by mass)[37] to produce a strong construction material.

We rely on gate-to-gate life cycle data from Kline (2005), which relies on survey data from operations in the Southeastern U.S.[38] To remain consistent with other pathways in this analysis, we rely on GREET data for forest residue handling and transportation emissions. We compared results with published cradle-to-gate LCA results for conventional OSB production (from harvested wood feedstock, rather than residues).[37] Despite differences in upstream processes and our exclusion of packaging and handling after production, we find similar results. Kline (2005) assumes a feedstock carbon content of 51.3%. We recalculate the carbon mass-balance to be consistent with a carbon content of 50.3%, as in GREET and our other forest residue pathway. Finally, there are roughly 16 kg of wood feedstock reported as unaccounted in Kline (2005). This unaccounted portion is a function of the mass balance assumptions made in the source literature and is highly sensitive to those assumptions. We add this material to the final mass of the OSB product. This adjustment is for internal consistency in carbon accounting and the mass difference is within the variance of OSB product mass.

**Table S25** – OSB data sources

| Process | LCI Source |
|---|---|
| Feedstock characteristics, collection, and transport | GREET.net 2018[13] |
| Gate to Gate OSB process emissions | Kline (2005)[38] |
| Fossil fuel inputs (upstream) and supply chain transportation emissions | GREET.net 2018 |
| PF Resin | Wilson (2010)[39] |
| MDI Resin | Franklin Associates (2011)[40] |
| Slack Wax, at plant, US SE | NREL / USLCI – Federal LCA Commons[41] |
| Co-product EOL | Offsite combustion for energy assumed / No displacement credits |

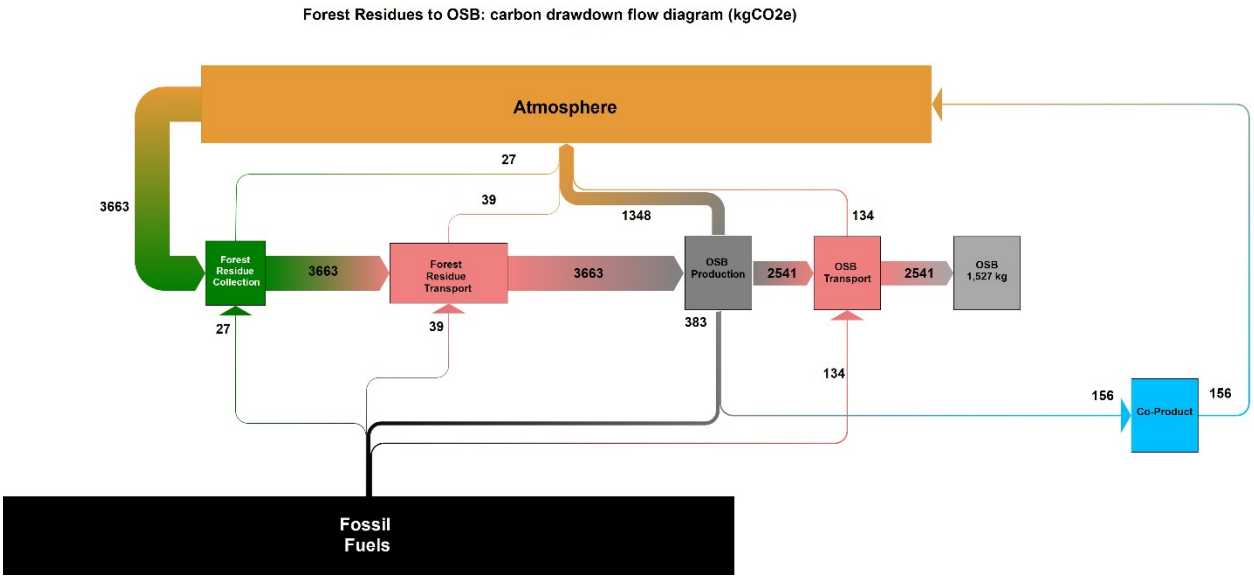


**Fig. S9** - Carbon flow through forest residues to OSB system as $CO_2e$ per tonne of feedstock. Embodied fossil emissions as well as upstream fossil emissions associated with production inputs are included in the flow diagram at the point where those inputs enter the production process. Thus, fossil emissions exiting a box in the diagram include both onsite emissions and emissions associated with upstream production of inputs. Note that carbon in methane and carbon monoxide emissions are not shown in this figure. These emissions account for the balance of carbon in the feedstock.

*Forest Residue Collection*

Forest residue collection is assumed to take place in Northern California. The residue travels 90 miles by heavy duty truck to the OSB mill. The forest residue is assumed to be 50.3% carbon by mass which is equivalent to roughly 1,844 kg of atmospheric $CO_2$/t of feedstock. Approximately 1.99 tonnes of forest residue are equivalent to the functional unit.

*OSB production from forest residues*

We assume a hypothetical OSB production facility located in Northern California.[42] Since OSB is highly standardized product due to building codes and regulations, we assume that the on

relevant differences between OSB production in California as opposed to the Southeastern U.S. will be the emissions intensity of energy sources and the end-of-life disposition of waste co-products. The OSB production process involves feedstock handling, flaking of logs, drying and screening, blending, mat formation and pressing, and finishing. In addition, heat is required for emissions control (combustion of VOCs). The process requires about 235 kW of electricity to process 1 tonne of forest residues. Electricity is assumed to have the emissions intensity of the average California distributed grid mix. Onsite wood fuel provides 89.6% (or 4,764 MJ per ton of residues) of the onsite heat energy requirement. The remainder of heat energy comes from natural gas, LPG, and fuel oil. About 80% of the heat energy requirement is used in the drying phase. Other heat requirements include pressing and emissions control. Onsite emissions for fossil fuels are taken from Kline (2005). Upstream emissions for fossil fuel production use North American values from the GREET model. Fossil fuels are also required for onsite material handling equipment. See Kline (2005) for additional details. In addition to wood feedstock, 25 kg of PF resin, 5 kg of MDI resin, and 11 kg of slack wax per ton of forest residue processed. The data sources for upstream emissions from these inputs are listed in **Table S25**.

*OSB Co-products*

The OSB process creates 26 kg of bark mulch, 11 kg of fines, and 6 kg of dust and scrap per ton of feedstock processed. For simplicity, this small amount of co-product is assumed to be combusted offsite. The emissions are biogenic, ultimately yielding no contribution the overall emissions intensity. We do not assign emissions credits for displacement of energy products.

*OSB End-of-life*

We do not attempt to calculate emissions from transportation of OSB to point-of-sale or point-of-use. Additional end-of-life assumptions for OSB are detailed in S.I 1.3 and 2.4.2.

### S2.6.1 Forest residue to OSB results

Life cycle OSB greenhouse gas emissions at the facility gate are -1,806 $kgCO_2e/tC$. Photosynthetic drawdown in the feedstock is 3,663 $kgCO_2/tC$ of forest residue (see **Fig. S9),** In **Table S26**, process and transportation $CO_2$ emissions total 1548 $kgCO_2/tC$. Of those emissions, 964 $kgCO_2/tC$ is biogenic, mostly from combustion of wood for heat energy, with a smaller portion arising from the combustion of VOCs as a result of abatement measures. 2,541 $kgCO_2/tC$ is sequestered in the final OSB product. An additional 156 $kgCO_2e/tC$ is sequestered in the wood co-products (bark, fines, waste), but it is ultimately assumed to be released via combustion offsite. The net $CO_2$ balance before consideration of non-$CO_2$ GHGs is -1,958 $kgCO_2/tC$.

**Table S26** - Life cycle $CO_2$ of forest residue converted to OSB. Where "Process Emissions" are indicated, this includes emissions occurring onsite at the farm or facility such as stack emissions or nitrogen cycling in the field. "Upstream Emissions" include everything else, e.g. emissions from electric grid, embodied emissions in chemical inputs, extraction and refining emissions associated with fuels.

| Life cycle emissions per 1 tonne C in feedstock |
|---|

| | | |
|---|---|---|
| **Products** | | |
| Oriented Strand Board (Mass basis) | 1526.88 | kg |
| Oriented Strand Board (Functional Unit Basis) | 2.57 | units |
| **$CO_2$ Emissions** | | |
| Process Emissions (Forest Residue Collection) | 22.43 | kg |
| Upstream Emissions (Forest Residue Collection) | 4.09 | kg |
| Forest Residue Transport | 38.95 | kg |
| Process Emissions (OSB Production) | 1078.22 | kg |
| Upstream Emissions (OSB Production) | 269.52 | kg |
| OSB Transport | 134.41 | kg |
| Total Emissions | **1547.61** | **kg** |
| Biogenic Credit (OSB Production) | -964.70 | kg |
| $CO_2$ in Co-Products | -156.14 | kg |
| $CO_2$ Sequestered in OSB Wood | -2541.20 | kg |
| Total w/ Biogenic Credit and Product Sequestration | **-2114.43** | **kg** |
| End-of-Life (Co-product combustion) | 156.14 | kg |
| Total Cradle to Grave Emissions | **-1958.29** | **kg** |

When the added impact of non-$CO_2$ GHG emissions is considered, as shown in **Table S27**, the final cradle-to-gate emissions total -1,806 kg$CO_2$e/tC.

**Table S27** - Non-$CO_2$ GHG emissions for OSB production

| **Non-$CO_2$ GHG Emissions and Total Life cycle $CO_2$e** | | |
|---|---|---|
| | | |
| $CH_4$ (Process) x 28 $CO_2$e | 100.82 | kg |
| $N_20$ (Process) x 265 $CO_2$e | 51.60 | kg |
| **Non-$CO_2$ GHGs (in $CO_2$e)** | **152.41** | **kg** |
| **Life Cycle $CO_2$e (w/ capture)** | **-1805.87** | **kg** |

### S2.6.2 OSB drawdown over 100; 1,000; and 10,000 years

Here we combine cradle-to-gate emissions for OSB production with the sequestration models described in S.I. 1.3 to estimate the long-term sequestration benefit of the conversion pathway. At $t = 0$, 693 kgC (2.541 kg$CO_2$/tC) is sequestered in the OSB product.

Per the sequestration functions described by Eq. 16 through Eq. 20, the carbon remaining in OSB at 100; 1,000; and 10,000 years is estimated. The quantity of OSB carbon emitted at $t$ is calculated by Eq. 21 and Eq. 22. The quantity of $CO_2$ and $CH_4$ emissions from energy production and landfill emissions at each time $t$ is calculated by Eq. 23 and Eq. 25 in the case of a landfill that

flares fugitive methane emissions. The emissions over time for the flaring case are shown in **Table S28**.

**Table S28** – OSB Flaring case emissions (representative case in bold)

| Case | Emission | 100 years (kg $CO_2$e/t) | 1,000 years (kg $CO_2$e/t) | 10,000 years (kg $CO_2$e/t) |
|---|---|---|---|---|
| OSB (product C) optimistic | $CO_2$ (energy) | 342.37 | 760.50 | 762.36 |
| | $CO_2$ (landfill) | 1.40 | 11.06 | 11.11 |
| | $CH_4$ (landfill) | 2.03 | 16.09 | 16.15 |
| **OSB (product C) moderate** | **$CO_2$ (energy)** | **468.79** | **762.31** | **762.36** |
| | **$CO_2$ (landfill)** | **142.80** | **346.46** | **346.50** |
| | **$CH_4$ (landfill)** | **207.71** | **503.95** | **504.00** |
| OSB (product C) pessimistic | $CO_2$ (energy) | 682.14 | 762.36 | 762.36 |
| | $CO_2$ (landfill) | 385.7 | 515.23 | 515.23 |
| | $CH_4$ (landfill) | 561.02 | 749.43 | 749.43 |

The full emissions profile for OSB production (moderate case) assuming that landfills flare methane emissions is shown in **Fig. S10**. Cradle-to-gate emissions are -1806 kg$CO_2$e/tC. At 100 years, 55% of the original drawdown remains. This falls to 11% at 1,000 and 10,000 years.

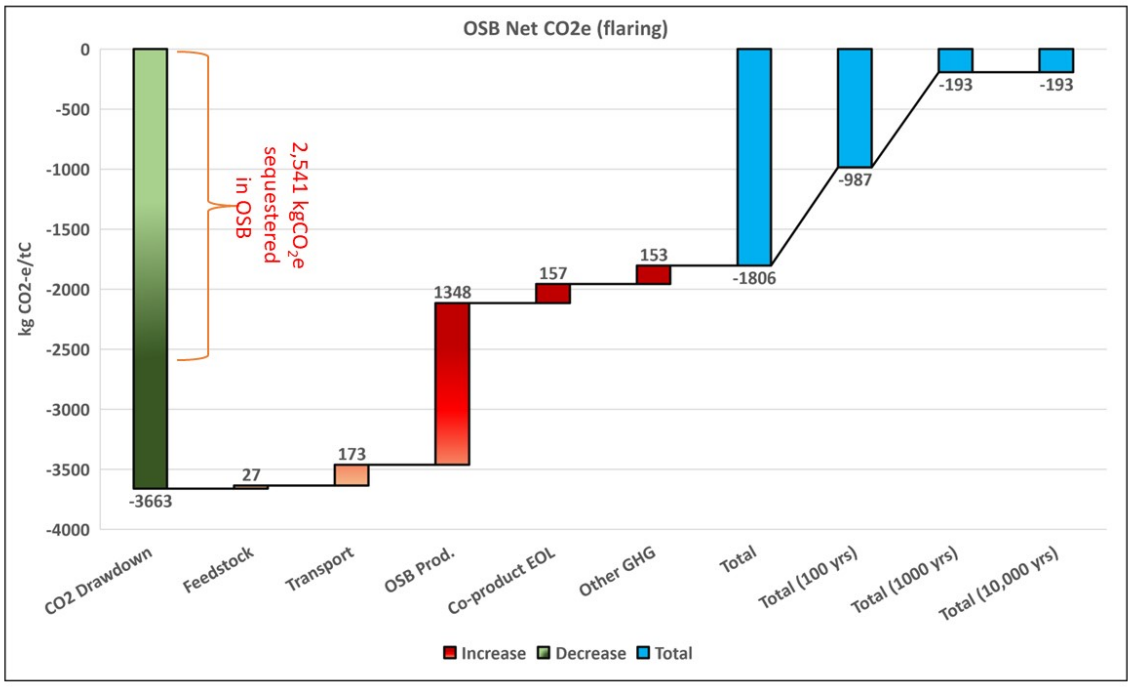


**Fig. S10** – OSB drawdown over 10,000 years (moderate case/flared landfills). Note that in the waterfall diagrams, green and red bars represent magnitudes of drawdown and emissions subsequent to the initial drawdown in biomass. The blue bars represent totals. The sum of all red and green bars is equal to the first blue bar.

For the scenario where landfills do not flare methane emissions, the quantity of $CO_2$ and $CH_4$ emissions from energy production and landfill emissions at each time $t$ is calculated by Eq. 24 and Eq. 26. The emissions over time for the no-flaring case are shown in **Table S29.**

**Table S29** – OSB non-flaring case emissions (representative case in bold)

| Case | Emission | 100 years (kg $CO_2$e/t) | 1,000 years (kg $CO_2$e/t) | 10,000 years (kg $CO_2$e/t) |
|---|---|---|---|---|
| OSB (product C) optimistic | $CO_2$ (energy) | 342.37 | 760.50 | 762.36 |
| | $CO_2$ (landfill) | 0.80 | 6.32 | 6.35 |
| | $CH_4$ (landfill) | 8.13 | 64.36 | 64.63 |
| **OSB (product C) moderate** | **$CO_2$ (energy)** | **468.79** | **762.31** | **762.36** |
| | **$CO_2$ (landfill)** | **81.60** | **197.98** | **198.00** |
| | **$CH_4$ (landfill)** | **830.82** | **2015.79** | **2016.02** |
| OSB (product C) pessimistic | $CO_2$ (energy) | 682.14 | 762.36 | 762.36 |
| | $CO_2$ (landfill) | 220.40 | 294.42 | 294.42 |
| | $CH_4$ (landfill) | 2244.09 | 2997.70 | 2997.70 |

The full 10,000-year (moderate case) emissions profile of the OSB pathway assuming that landfills do not manage methane emissions is shown in **Fig. S11**. Cradle-to-gate emissions are -1,806 kg$CO_2$e/tC. At 100 years 24% of the original drawdown benefit remains. At 1,000 and 10,000 years, the pathway yields significant net emissions. This is primarily due to high GWP of methane emissions in the landfill.

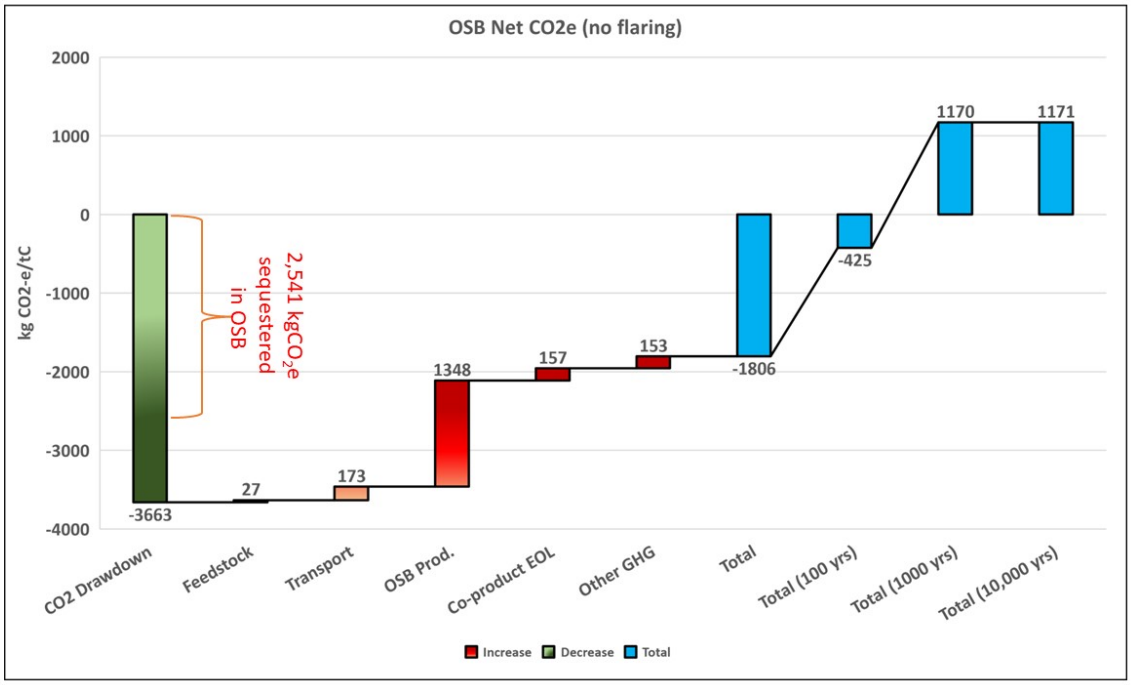


**Fig. S11** - OSB drawdown over 10,000 years (moderate case/unflared landfills). Note that in the waterfall diagrams, green and red bars represent magnitudes of drawdown and emissions subsequent to the initial drawdown in biomass. The blue bars represent totals. The sum of all red and green bars is equal to the first blue bar.

### S2.6.3 OSB counterfactual selection

From the meta-analysis by Sathre and O'Connor, we draw our range of displacement factors from **Table 2**: *Low, middle, and high estimates of displacement factors of wood product substitution (tC emission reduction per tC of additional wood products used) based on data from 21 studies.* We select only consider the subset of estimates from the literature that explicitly involve "building" construction, i.e. scenarios where OSB is a plausible wood substitute. We selected the lowest and highest displacement factors from the middle range column of estimates to arrive at 0.4 to 6.0 tC diplaced per tonne of wood C utilized. In our manuscript, we report these values to $tCO_2$/t wood C (1.5 – 22.0 $tCO_2$/C).

## References


1. Alcalde, J. *et al.* Estimating geological CO2 storage security to deliver on climate mitigation. *Nat. Commun.* **9**, (2018).
2. U.S. Environmental Protection Agency. Plastics: Material-Specific Data. *Facts and Figures about Materials, Waste and Recycling* https://www.epa.gov/facts-and-figures-about-materials-waste-and-recycling/plastics-material-specific-data (2020).
3. Stahmer, M. Polyethylene - the optimum gas pipe material? [technical memo]. **4130**, 1–2 (2008).
4. Colt, J., Driscoll, W. & Freed, R. Work Assignment 239, Task 2: Carbon Sequestration in Landfills [Memorandum]. (1995).
5. U.S. Environmental Protection Agency. Advancing Sustainable Materials Management: 2014 Fact Sheet Assessing Trends in Material Generation, Recycling, Composting, Combustion with Energy Recovery and Landfilling in the United States. (2014).
6. U.S. Environmental Protection Agency Office of Resource Conservation. *Documentation for Greenhouse Gas Emission and Energy Factors Used in the Waste Reduction Model (WARM) - Containers, Packaging, and Non-Durable Goods Materials Chapters*. (2016).
7. Albertsson, A. C. The shape of the biodegradation curve for low and high density polyethenes in prolonged series of experiments. *Eur. Polym. J.* **16**, 623–630 (1980).
8. Ghatge, S., Yang, Y., Ahn, J.-H. & Hur, H.-G. Biodegradation of polyethylene: a brief review. *Appl Biol Chem* **63**, 27 (2020).
9. Shah, A. A., Hasan, F., Hameed, A. & Ahmed, S. Biological degradation of plastics: A comprehensive review. *Biotechnology Advances* vol. 26 246–265 (2008).
10. Chamas, A. *et al.* Degradation Rates of Plastics in the Environment. *ACS Sustain. Chem. Eng.* **8**, 3494–3511 (2020).
11. Skog, K. E. Sequestration of carbon in harvested wood products for the United States. *For. Prod. J.* **58**, 56–72 (2008).
12. Lee, U., Han, J. & Wang, M. Evaluation of landfill gas emissions from municipal solid

waste landfills for the life-cycle analysis of waste-to-energy pathways. *J. Clean. Prod.* **166**, 335–342 (2017).

13. Wang, M. *et al.* Greenhouse gases, Regulated Emissions, and Energy use in Transportation Model ® (2018 .Net). (2018) doi:10.11578/GREET-Net-2018/dc.20200803.8.

14. Levasseur, A., Lesage, P., Margni, M., Deschĕnes, L. & Samson, R. Considering time in LCA: Dynamic LCA and its application to global warming impact assessments. *Environ. Sci. Technol.* **44**, 3169–3174 (2010).

15. Stewart, W. C. & Nakamura, G. M. Documenting the full climate benefits of harvested wood products in northern california: Linking harvests to the us greenhouse gas inventory. *For. Prod. J.* **62**, 340–353 (2012).

16. Intergovernmental Panel on Climate Change (IPCC). 2006 IPCC Guidelines for National Greenhouse Gas Inventories: Vol 5 Chapter 3 Solid Waste Disposal. *2006 IPCC Guidel. Natl. Greenh. Gas Invent.* **5**, 6.1-6.49 (2006).

17. Gurwick, N. P., Moore, L. A., Kelly, C. & Elias, P. A Systematic Review of Biochar Research, with a Focus on Its Stability in situ and Its Promise as a Climate Mitigation Strategy. *PLoS One* **8**, e75932 (2013).

18. Singh, B. P., Cowie, A. L. & Smernik, R. J. Biochar carbon stability in a clayey soil as a function of feedstock and pyrolysis temperature. *Environ. Sci. Technol.* **46**, 11770–11778 (2012).

19. Enders, A., Hanley, K., Whitman, T., Joseph, S. & Lehmann, J. Characterization of biochars to evaluate recalcitrance and agronomic performance. *Bioresour. Technol.* **114**, 644–653 (2012).

20. Wang, J., Xiong, Z. & Kuzyakov, Y. Biochar stability in soil: meta-analysis of decomposition and priming effects. *GCB Bioenergy* **8**, 512–523 (2016).

21. Santos, F., Torn, M. S. & Bird, J. A. Biological degradation of pyrogenic organic matter in temperate forest soils. *Soil Biol. Biochem.* **51**, 115–124 (2012).

22. Goodwin, J., Gillenwater, M., Romano, D. & Radunsky, K. Chapter 1 Introduction To National Ghg Inventories. *Refinement to 2006 IPCC Guidel. Natl. Greenh. Gas Invent.* **1**, 1–22 (2019).

23. Searchinger, T. *et al.* Use of U.S. croplands for biofuels increases greenhouse gases through emissions from land-use change. *Science (80-. ).* **319**, 1238–1240 (2008).

24. Levasseur, A., Lesage, P., Margni, M. & Samson, R. Biogenic Carbon and Temporary Storage Addressed with Dynamic Life Cycle Assessment. *J. Ind. Ecol.* **17**, 117–128 (2013).

25. Sanderson, M. A., Adler, P. R., Boateng, A. A., Casler, M. D. & Sarath, G. Switchgrass as a biofuels feedstock in the USA. *Can. J. Plant Sci.* **86**, 1315–1325 (2006).

26. Montgomery, T. D., Han, H. S. & Kizha, A. R. Modeling work plan logistics for

centralized biomass recovery operations in mountainous terrain. *Biomass and Bioenergy* **85**, 262–270 (2016).

27. Kanniche, M. *et al.* Pre-combustion, post-combustion and oxy-combustion in thermal power plant for CO2 capture. *Appl. Therm. Eng.* **30**, 53–62 (2010).

28. Pedroso, G. M. *et al.* Switchgrass is a promising, high-yielding crop for California biofuel. *Calif. Agric.* **65**, 168–173 (2011).

29. Rhodes, J. S. & Keith, D. W. Biomass Energy with Geological Sequestration of CO2: Two for the Price of One? *Greenh. Gas Control Technol. - 6th Int. Conf.* **II**, 1371–1376 (2003).

30. National Energy Technology Laboratory. *Cost of Capturing CO2 from Industrial Sources*. *Doe/Netl-2013/1602* https://sequestration.mit.edu/pdf/2013_Summers_Capture_Costs_Industrial_Sources.pdf (2014).

31. McCoy, S. T. & Rubin, E. S. An engineering-economic model of pipeline transport of CO2 with application to carbon capture and storage. *Int. J. Greenh. Gas Control* **2**, 219–229 (2008).

32. U.S. Department of Energy. *2016 billion-ton report: Advancing domestic resources for a thriving bioeconomy, Volume 1: Economic Availability of Feedstocks*. (2016) doi:10.1089/ind.2016.29051.doe.

33. Heath, L. S., Birdsey, R. A., Row, C. & Plantinga, A. J. Carbon pools and fluxes in U.S. forest products. in *Forest Ecosystems, Forest Management and the Global Carbon Cycle* 271–278 (Springer Berlin Heidelberg, 1996). doi:10.1007/978-3-642-61111-7_25.

34. Qin, Z., Dunn, J. B., Kwon, H., Mueller, S. & Wander, M. M. Influence of spatially dependent, modeled soil carbon emission factors on life-cycle greenhouse gas emissions of corn and cellulosic ethanol. *GCB Bioenergy* **8**, 1136–1149 (2016).

35. Mermertaş, M. & Germirli Babuna, F. Life Cycle Environmental Impact Analysis of HDPE Packaging Materials for Different Disposal Options. in 55–61 (Springer, Cham, 2019). doi:10.1007/978-3-319-95888-0_5.

36. Puettmann, M., Wilson, K. & Oneil, E. *Life cycle assessment of biochar from post-harvest forest residues (Draft Report)*. (2017).

37. Puettmann, M., Oniel, E., Kline, E. & Johnson, L. *Cradle to Gate Life Cycle Assessment of Oriented Strandboard Production from the Southeast*. (2012).

38. Kline, D. E. Gate-to-gate life-cycle inventory of oriented strandboard production. *Wood Fiber Sci.* **37**, 74–84 (2005).

39. Wilson, J. B. Life-cycle inventory of formaldehyde-based resins used in wood composites in terms of resources, emissions, energy and carbon. *Wood Fiber Sci.* **42**, 125–143 (2010).

40. Franklin Associates. Cradle-To-Gate Life Cycle Inventory of Nine Plastic Resins. *Am. Chem. Counc.* 1–198 (2011).

41. National_Renewable_Energy_Laboratory/USLCI | LCA Collaboration Server. https://www.lcacommons.gov/lca-collaboration/National_Renewable_Energy_Laboratory/USLCI/dataset/PROCESS/2c79b9d3-e5f9-34a8-990e-b7d6f9e4dd08.

42. Beck Group. *California Assessment of Wood Business Innovation Opportunities and Markets ( CAWBIOM )*. (2015).